USING UNMANNED AIRCRAFT SYSTEMS FOR CONSTRUCTION VERIFICATION, VOLUME CALCULATIONS, AND FIELD INSPECTION

By

Andres Leonardo Acero Molina

July, 2023

Director of Thesis: Yilei Huang, Ph.D.

Major Department: Construction Management

The construction field is one of the most variable industries due to continuous technological advances impacting this industry. Innovative research is currently being applied to construction disciplines such as surveying and design in order to optimize labor, costs, and time. However, there remains a need to improve productivity and safety for construction projects. Unmanned Aircraft Systems (UAS) have been implemented as a means to offer a new alternative for onsite data collection, due to the limitations of traditional surveying methods such as GPS and total station, which are usually an exhausting manual process. The main goal of this research was to use UAS technologies to improve the efficiency of construction surveying and inspection activities. Different UAS flights were performed to verify a variety of measurements obtained from building plans. The comparison of volume calculations for an aggregate pile was determined using full point cloud data to generate a 3D model, which was compared with the 3D models obtained using GPS point and extracted point cloud. The model obtained using the full point cloud data showed greater accuracy as compared with the traditional surveying models since its generated surface was more similar to the actual surface of the pile. Field inspection of a

bridge's typical structures was accomplished by using a point cloud model, as well as photogrammetric models under daylight and twilight conditions. The highest linear measurement variation for field inspection was almost 1/3 foot in a 33-foot length. This outcome yielded a generally acceptable degree of accuracy for inspection tasks. In addition, photogrammetric models can provide high-quality pictures for visual inspection of other bridge components, such as the assessment of the Rip Rap located at the beginning of the bridge selected for this research.

USING UNMANNED AIRCRAFT SYSTEMS FOR CONSTRUCTION VERIFICATION, VOLUME CALCULATIONS, AND FIELD INSPECTION

A Thesis

Presented To the Faculty of the Department of Construction Management

East Carolina University

In Partial Fulfillment of the Requirements for the Degree

Master of Science in Construction Management

by

Andres Leonardo Acero Molina

July, 2023

USING UNMANNED AIRCRAFT SYSTEMS FOR CONSTRUCTION VERIFICATION, VOLUME CALCULATIONS, AND FIELD INSPECTION

By

Andres Leonardo Acero Molina

APPROVED BY:

Director of Thesis _____

Yilei Huang, Ph.D.

Committee Member _____

Mostafa Namian, Ph.D.

Committee Member _____

Tianjiao Zhao, Ph.D.

Committee Member _____

Zhen Zhu, Ph.D.

Chair of the Department of Construction Management _____

George Wang, Ph.D.

Interim Dean of the Graduate School _____

Kathleen Cox, Ph.D.

ACKNOWLEDGEMENTS

Words cannot express my gratitude to my advisor Dr. Yilei Huang for always being there when I needed his support, reviewing my progress constantly, and guiding me through my MSc studies. Special thanks to each member of my thesis committee for addressing this research by providing their knowledge and expertise.

I would like to express my deepest appreciation to Dr. MaryAnn Stone for her editing help, extensive feedback sections, and moral support. Many thanks to the staff members of the Department of Construction Management at ECU for their help during this journey.

This endeavor would not have been possible without my family's support. Their belief in me has been an incredible motivation to work hard in order to accomplish my goals.

TABLE OF CONTENTS

LIST OF TABLES

LIST OF FIGURES

CHAPTER 1 INTRODUCTION

1.1 Background

The construction industry comprises a vast variety of fields which includes architecture, engineering, manufacturing, fabrication, project management, inspection, and facility management. It is one of the largest industries in the world. Although it is considered a non-intensive technological industry, new techniques and methods to improve productivity and safety have increasingly been employed during the last decade. These techniques include the transition from 2D Computer-Aided Design (CAD) to 3D Building Information Modeling (BIM), and from traditional manual operations to robotic-aided and automated systems. Unmanned Aircraft Systems (UAS) is another of these innovative technologies due to their unparalleled efficiency over conventional methods.

Construction professionals have implemented UAS for various tasks such as inspection, surveying, safety, monitoring, etc. Different types of imaging and sensing UAS technologies have been implemented to obtain geographical and surveying data under specific project conditions such as red, green, and blue (RGB) color images, monochrome LIDAR point clouds, and thermal imagery. UAS are widely known under different names, such as drones and Unmanned Aerial Vehicles (UAV) (Siebert and Teizer 2014).

1.2 Problem Statement

UAS has been implemented in construction research projects to explore better techniques instead of conventional methods to get data on worksites. In current construction projects, conventional surveying with total stations and GPS is typically a manual and repetitive process with extensive time and labor efforts in the field. Additionally, certain field inspection tasks can

expose construction workers to various types of risks and hazards that are related to site and weather conditions. Based on the mentioned previously, the construction field has been trying to enhance techniques and methods to enhance accuracy, costs, and time indicators in projects. UAS assessment for different tasks in construction is one of the innovative alternatives in order to benefit the efficiency of projects.

1.3 Goal and Objectives

The main goal of this research is to use UAS technologies to improve the efficiency of construction surveying and inspection activities. The objectives to address this goal were:

- Identify the accuracy of linear dimensions through photogrammetric and point cloud models;
- Determine the approach of volume calculation and compare the differences between the values obtained from photogrammetric models (DJI Terra and Drone Deploy) and point cloud model (Autodesk Civil 3D); and
- Investigate the workflow of how to use the UAS to do inspections of data known from build plans of different structures.

1.4 Thesis Organization

This thesis is divided into eight chapters: (1) Introduction; (2) Literature Review; (3) Methodology; (4) Verification of Linear Dimensions; (5) Comparison of Volume Calculations; (6) Inspection of Bridge Structures; (7) Discussions; and (8) Conclusions and Recommendations.

Chapter 1 presents a background of UAS uses in construction; problem statement; and goals and objectives. Chapter 2 provides a literature review of the use of UAS in construction. Chapter 3 outlines the data collection and the methodology used. Chapters 4, 5, and 6 present the

results of different data obtained. Chapter 7 presents the discussion and analysis of the results, and Chapter 8 provides the overall benefits, limitations, and recommendations resulting from this research.

CHAPTER 2 LITERATURE REVIEW

2.1 Introduction

Extensive research using UAS in the construction field has been utilized to improve efficiency in cost, money, labor, and accuracy (Dupont et al. 2017). Professionals involved in the engineering field have focused their research with UAS for surveying, inspection, safety, and operations. In engineering, other research has analyzed the implementation of UAS in construction management roles and applications (Li and Liu 2019).

While thousands of UAS-related research studies have been performed, only those directly contributing to construction applications are considered and included in this document. The reviewed literature was collected from a selection of academic journals and conferences in the field of civil engineering and construction management, as listed in Table 1. A publication timeframe of 2016-2021 was chosen for the journal papers, and a timeframe of 2018-2021 was used for the conference proceedings. The 95 reviews included 82 journal papers and 13 conference papers. Journal papers on Automation in Construction accounted for about a quarter of the reviewed papers.

Table 1. Journals and Conferences Selected for Data Collection of the Literature

Journal Name	No. of Papers
Automation in Construction	25
Journal of Computing in Civil Engineering	16
Transportation Research Record	8
Journal of Management in Engineering	6
Journal of Bridge Engineering	5
Journal of Surveying Engineering	5
Journal of Construction Engineering and Management	3
Journal of Geotechnical and Geoenvironmental Engineering	3
Remote Sensing	3
Other Journals	8
Total Journal Papers	82
Conference Name	**No. of Papers**
ASCE Construction Research Congress	6
Associated Schools of Construction Annual International Conference	3
ASCE International Conference on Computing in Civil Engineering	2
Other Conferences	2
Total Conference Papers	13

The year of publication and the country corresponding to the reviewed published literature were also analyzed. As demonstrated in Figure 1, the number of published papers has increased steadily since 2016, closely following a linear regression with an annual increment of roughly six. Figure 2 illustrates the distribution of countries for the reviewed literature. While about half of the studies were performed in the United States, around 10% were from Europe and China, respectively; and 5% were from South Korea and Canada, respectively. The remaining studies were carried out in other countries including Australia, Saudi Arabia, and Singapore.

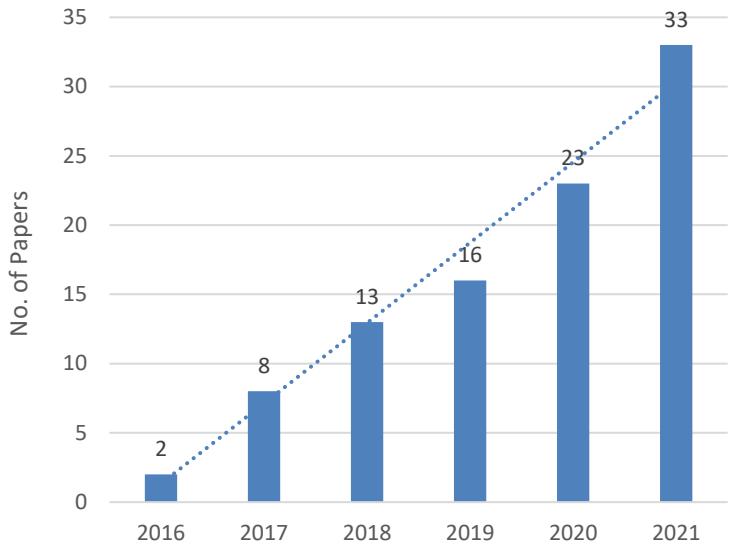

Figure 1. Year of Publication of the Reviewed Literature

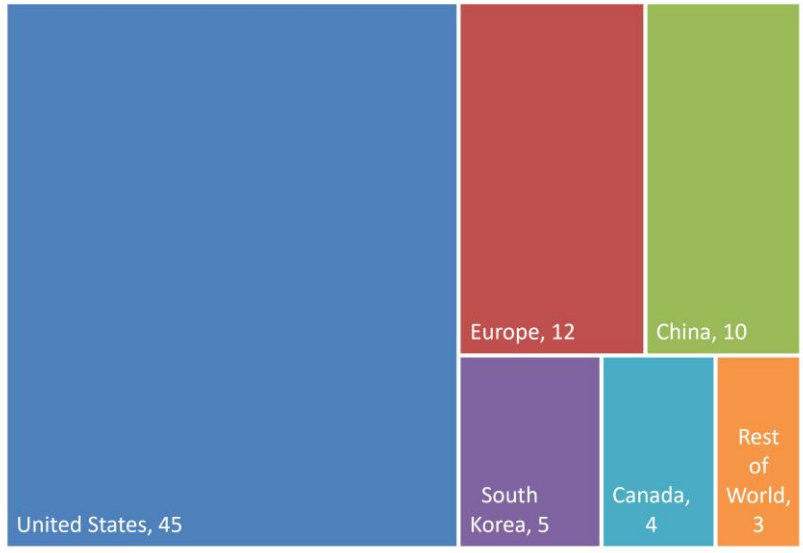

Figure 2. Country Corresponding to the Reviewed Published Literature

2.2 Overview

All the reviewed papers were classified based on their main goals, which could be either for construction uses or UAS uses. Although the main topic of this paper is focused on direct

construction uses, many of the reviewed studies investigated a particular aspect of UAS use for construction activities, such as algorithms for aerial imaging processing, frameworks for carrying out construction tasks, the operations for performing construction tasks using a UAS, etc. As a result, the literature was classified into categories of UAS use. In total, 65 papers dealing with construction uses were identified and reviewed, while 32 papers regarding UAS uses were analyzed. All reviewed literature was then further categorized, based on their sensing technology types and targeted structure types, as a means to illustrate the connection between the research topics, sensing technologies, and structure types.

2.2.1 Topics

The reviewed literature was grouped together based on their research topics in both the UAS and construction categories, as listed in Table 2. In the category of UAS uses, about one-third of the papers developed new algorithms for aerial imaging and point cloud processing, followed by a quarter of the papers on UAS applications and UAS operations for construction tasks, respectively. In the category of construction uses, over half of the literature focused on the topic of inspection while a third studied construction surveying with UAS. Research topics less focused on included UAS safety and training as well as construction monitoring and construction methods with UAS.

Table 2. A Summary of Identified Research Topics of the Reviewed Literature

Category	Topic	No. of Papers
UAS Uses	Algorithm	11
	Applications	7
	Operations	7
	Framework	4
	Safety	1
	Training	1
Construction Uses	Inspection	36
	Surveying	20
	Safety	5
	Monitoring	2
	Methods	1

2.2.2 Technologies

The review was then categorized by the types of sensing technology applied, as illustrated in Figure 3. Among the 71 publications which specified the sensor types, two-thirds applied RGB photogrammetry, indicating that color images were the dominant data type for UASs. Around a quarter of the studies employed LIDAR, suggesting that despite being more costly than imaging cameras, LIDAR sensors were still a popular choice for research studies in the construction field. Other types of sensing technologies included thermal imaging, video footage, and multispectral images, accounting for one-ten combined. A few studies applied multiple types of sensors at the same time and were therefore included in each of the sensor categories.

In addition to the sensing methods, other advanced technologies have also been applied together with UASs, such as deep learning, neural network, Virtual Reality/ Augmented Reality (VR/AR), and Unmanned Ground Vehicles (UGVs). The connections of these technologies in particular research topics suggested the optimal selection of research methods and equipment. By performing a text data mining of the title wording of the reviewed literature. Figure 4 illustrates the typical connection links between the research topics, sensing methods, structure types, and

other advanced technologies. For example, images were frequently used for detection and deep learning, and inspection was typically an automated process for buildings. Most studied topics, including images, inspection, and bridges, were closely connected to 3D technologies.

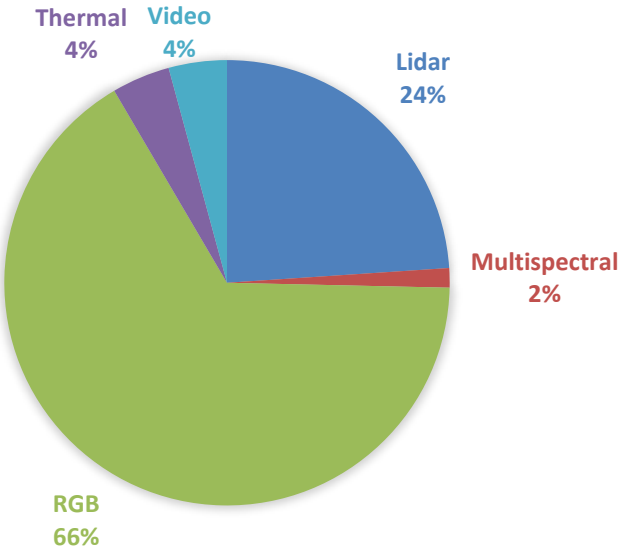

Figure 3. Frequency of the Type of UAS Sensors Applied in the Reviewed Literature

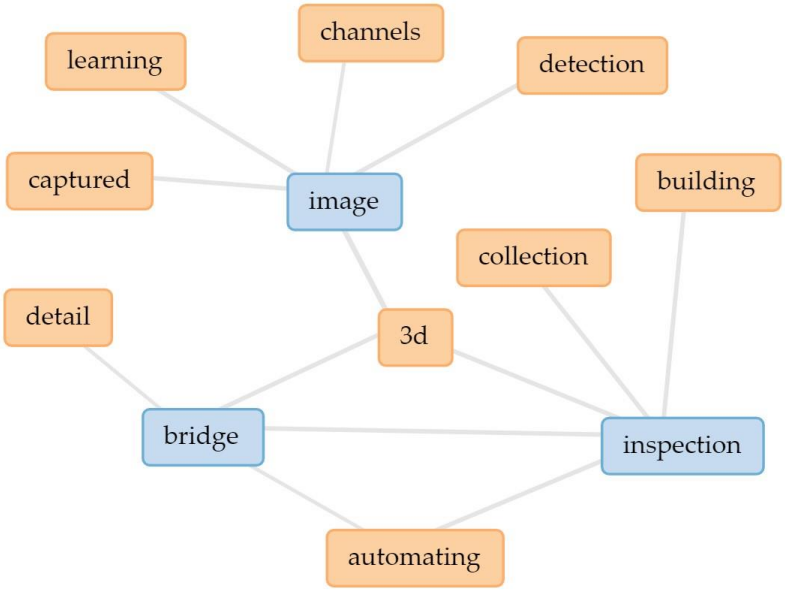

Figure 4. Links for the Most Frequent Title Words of the Reviewed Literature

2.2.3 Structure Types

In terms of targeted structure types studied by the reviewed literature, where 72 reviewed publications had specified, most of them had focused on sites and buildings, accounting for 29% and 24%, respectively, followed by roads and bridges at 17% and 15%, respectively, as illustrated in Figure 5. The remaining studied structure types included wetland, disaster, equipment, and dam, totaling a combined 15% of the reviewed literature.

Text data mining was performed again to provide a visual representation of the frequency of title wording of all reviewed literature. After removing the common words including UAS, aerial, unmanned, vehicle, drone, construction, and general words such as using, based, data, a cirrus of the most frequent 100 words in the titles of the reviewed literature is demonstrated in Figure 6 to represent the popularity of the title wording. It can be observed that image, inspection, 3D, bridge, and building are the most frequently appearing words in the literature titles, followed by photogrammetry, monitoring, detection, automated, mapping, and deep learning. Other noticeable title wording also included assessment, framework, LIDAR, point cloud, site, and road.

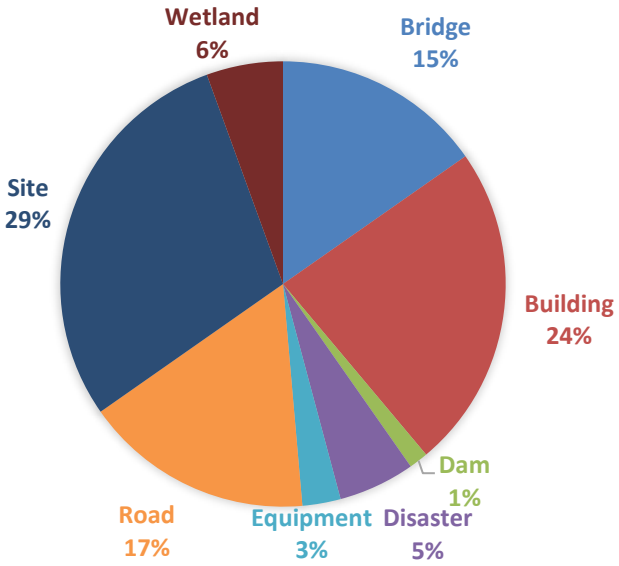

Figure 5. Frequency of the Structure Types Studied by UAS in the Reviewed Literature

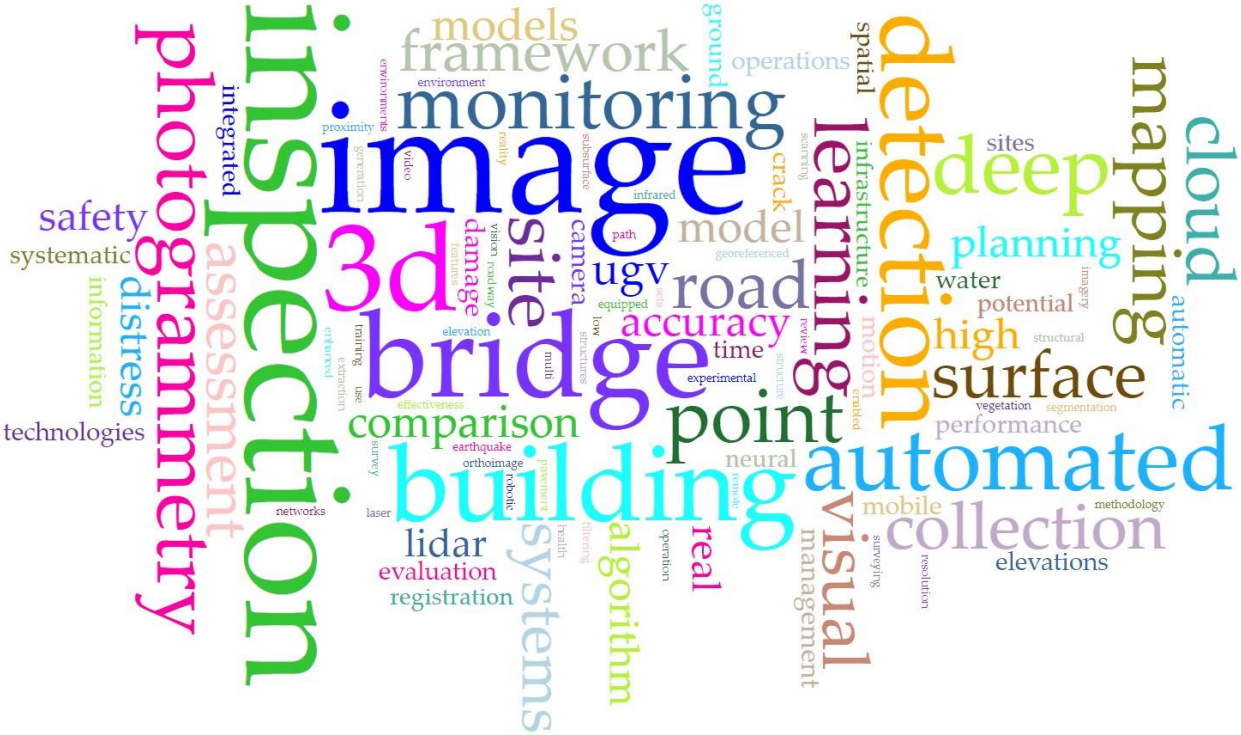

Figure 6. Cirrus for Most Frequent 100 Words in the Titles of the Reviewed Literature

2.3 UAS Uses

A total of 32 papers were classified in the category of UAS uses for construction, including specific topics in the areas of algorithms, applications, operations, and framework. Very few papers were found on the topics of safety and training and therefore were discussed together later.

2.3.1 Algorithm

Research studies focusing on the topic of algorithms include various algorithm methods, data collection, and software. For example, Bang et al. (2017) proposed a method to generate a panorama of a construction site by using an image-stitching technique with a focus on preprocessing. Future studies are required to bring this study to its full fruition. The mentioned deficiencies, such as misalignment and information loss, suggest a direction for future studies. Kamari and Ham (2018) constructed a generative model with an unlabeled visual dataset and used it to find construction-related frames in a big visual dataset from job sites. The contribution of this research was being able to focus on selective visual data. Practitioners will be able to spend less time browsing large amounts of visual data; and, rather, spend more time looking at how to leverage the visual data to facilitate decision makings in built environments.

Ham and Kamari (2019) proposed a new method to automatically retrieve photo-worthy frames containing construction-related contents that were scattered in collected video footage or consecutive images. The main contribution of this work was to automate construction visual data filtering and retrieving images that are valuable for documenting the status of construction job sites from video footage captured via UAVs.

Chen et al. (2020) introduced a model assembling framework for segmenting a 3D photogrammetry point cloud into top-level terrain elements (i.e., ground, human-made objects, and vegetation). Preprocessing and postprocessing methods were designed to overcome the data segmentation challenges posed by photogrammetric data-quality issues. Liu et al. (2020) proposed a deep learning-based deblurring model based on a Generative Adversarial Network (GAN) network. The methodology was designed to achieve a kernel-free deblurring of input crack images to support façade crack inspection. The model was built with a discriminator sub-model chained to a generator sub-model.

Bang and Kim (2020) proposed a methodology to generate time-spatial and visual context-based information from UAV-acquired data. This methodology for context-based construction information built a database considering time-spatial context and situational awareness, at a construction site from UAV-acquired data consisting of images and flight data. Ham et al. (2020) used three state-of-the-art object detectors: faster R-CNN, SSD, and R-FCN for vehicle detection. The hyperparameters of each detector were properly adjusted for the best performance in vehicle detection. Random mixing of all images did not guarantee high accuracy but rather showed a decrease in overall performance when other environments were added. Future research could include more detailed contexts, for example, night and evening lighting conditions, complex congestion crossings, and vehicle tracking.

Pi et al. (2021) contributed to the core body of knowledge by presenting a fully annotated dataset with the object classes including people, flooded areas, damaged and undamaged building roofs, cars, debris, vegetation, roads, and boats, and developed a host of convolutional neural networks (CNN) models for detecting and segmenting critical objects in the aerial footage of disaster sites. Wang and Li (2021) proposed a blur detection method for the crack image data

sets acquired by UAV and then classified the crack images based on visual information by throbyculating metrics and comparing it with other EAWD values from the same data set. The crack images were judged to be blurred or not.

Fu et al. (2021) optimized an object-based RF algorithm through multiple iterations and then used it for coarse classification. In this study, a new method was proposed for classifying a karst vegetation community based on UAV images, which provided technical support and theoretical reference for the protection and reasonable development of the Huixian karst wetland. Bianchi et al. (2021) outlined a use case for a data set and model to detect critical structural bridge details, providing context and vision for enhancing the autonomous UAV bridge inspection process. Four structural bridge details were chosen from the photos collected for this study, including bearings, cover plate terminations, gusset plates, and out-of-plane stiffeners.

2.3.2 Applications and Operations

Research studies focusing on UAV applications and operations are summarized here together in different aspects of on-site work, such as photography, monitoring, and site research. Irizarry and Costa (2016) presented an exploratory case study to identify potential applications of visual assets obtained from UAVs for construction management tasks. The main contributions of this paper were to improve the use of UAV-based visual assets for construction management tasks and to identify relevant opportunities to explore this emerging technology. Dupont et al. (2017) explored the potential of UAVs in linking BIM to the real world to improve productivity. They identified challenges to achieve this goal, in two main areas, namely the robotic challenge and the software and civil engineering challenge.

Adjidjonu and Burgett (2019) developed an experiment to test the accuracy of the deployment of Phantom 4 Pro in a 1,000-sf slightly-slope area. The use of one drone was a limitation of the study since different UAV camera specifications will have different results. Albeaino et al. (2019) classified all Architecture, Engineering, and Construction (AEC) industry-related UAV applications within the past decade, which extended the understanding of the current state of UAV implementation in the AEC domain and outlined relevant research trends in this setting. The methodology was focused on a structured analysis that reports topic-specific studies in a replicable, objective, and comprehensive manner.

Albeaino and Gheisari (2020) explored the current state of practice of UAV integration in construction from the industry professionals' viewpoint. Three main tasks were performed to accomplish the objectives of this study, namely the development of a survey instrument, data distribution and collection, and data screening and analysis. Asadi and Han (2020) proposed a mobile robotic system that integrates two mobile robots, a ground vehicle, and an aerial micro blimp. The key aspects of the development of this autonomous navigation system were efficient path planning, localization of both ground and aerial robots, and mapping of the surrounding environment.

Kim and Kim (2021) performed a tertiary study that consisted of three main steps: (1) selection of secondary review studies; (2) quality assessment (QA) of the selected studies; and (3) information synthesis based on tertiary review. The main contribution of this study was to increase the body of knowledge available regarding UAV applications and the current state of research on evidence-based tertiary reviews.

2.3.3 Framework

Various research studies have implemented different UAV frameworks. Zhou et al. (2018) explored a multidimensional framework from four dimensions: lifecycle, managed object, potential role, and stakeholder engagement. The proposed framework offered a thorough schema from four dimensions that increase the understanding of UAV functions and the potential for construction project management. This multidimensional framework was open to practitioners and researchers to expand the dimensions and supplement the scenarios of UAV applications. Shojaei et al. (2018) explored the viability of using a small and low-cost Unmanned Surface Vehicle (USV) as a stand-alone robotic agent and as a cooperative agent with UAVs. Another goal of this study was to provide proof of this concept for applications and the development of small and low-cost USVs similar to the current available UAVs.

Park et al. (2019) proposed a framework for the automated registration of UAV and Unmanned Ground Vehicle (UGV) point clouds using 2D local feature points in the images taken from UAVs and UGVs. This study conducted field experiments by varying the angles of the UAV camera to identify the optimal angle and detect sufficient points matching the images taken by the UGV. Kim et al. (2021) proposed a framework for inspecting runway design codes (RDCs) for airfields that rely on mosaic imagery. A fixed-wing UAV platform was deployed to capture aerial images of an airport testbed. The validation results showed that the framework had a high enough level of accuracy to measure pixel-based distances for RDC items that were comparable to the results of manual airport inspections.

2.4 Construction Uses

A total of 65 papers on construction uses were identified and reviewed, including topics on inspection and surveying. Very few papers were found on the topics of safety, monitoring, and methods and therefore were discussed together later.

2.4.1 Inspection

UAV uses in construction inspection have been the most implemented category in the reviewed literature. Zhou et al. (2016) grouped the photos collected during Hurricane Sandy to explore image-based 3D reconstruction for post-hurricane residential building damage assessment. One limitation of the research was that it was necessary to assume that the images were grouped by individual buildings, which simplified the reconstruction process since it is well-known that buildings tend to have similar local features. Omar and Nehdi (2017) explored the potential application of UAV Infrared Thermography for detecting subsurface delamination in concrete bridge decks. This application required neither traffic interruption nor physical contact with the deck being inspected. The proposed methodology allows post-flight data processing.

Eschmann and Wundsam (2017) analyzed the interregional usage of UAVs for infra-structural inspection as well as structural health monitoring (SHM). A major issue of this study was airborne sensor navigation, which faces accuracy problems due to factors such as sensor hardware specifications, atmospheric conditions, or infrastructure properties. Franke et al. (2017) presented the first documented use of small UAVs for reconnaissance of seismic-induced soil liquefaction and lateral spread following a major earthquake that happened in Chile in 2014. UAV-based remote sensing appeared to provide a sensible balance between acquisition/maintenance costs, portability, visibility, model resolution, and accuracy.

Seo et al. (2018) analyzed the effectiveness of UAVs as supplemental bridge inspection tools. The use of photogrammetry software allowed for a more comprehensive and detailed view of the damage. The UAV was able to identify a variety of damage types, including cracking, spalling, corrosion, and moisture on the bridge. Inzerillo et al. (2018) validated the use of innovative and low-cost technologies for road pavement analysis and for assessing their potential for improving the automation and reliability of distress detection. These UAV-SfM results are useful to understand the overall conditions of the state of a long stretch of road pavement by identifying the critical areas of the road surface where it is necessary to carry out a more detailed analysis.

Duque et al. (2018) evaluated the effectiveness of a UAV as a supplementary bridge damage quantification tool. The UAV operation presented some limitations caused mainly by unfavorable weather conditions, including wind speed, limited illumination, and image over- and under-exposure. Dorafshan et al. (2018) studied the feasibility of using UAVs for fatigue crack detection in bridges with fracture critical members (FCMs) through real-time and postflight visual inspection. Two FCM inspections of structures with known fatigue cracks demonstrated the ability of the UAV platform to identify fatigue cracks in the field. Bashmal et al. (2018) developed a Siamese-GAN method for cross-domain categorization in aerial vehicle images. The main objective was to obtain data coming from two different domains, namely labeled source and unlabeled target data.

Chen et al. (2019) proposed a systematic process for detecting and managing building anomalies based on drone-collected images. An overall data structure, data flow, and related processing techniques within this systematic process were defined and the outcome did support façade anomaly detection. Kim et al. (2019) introduced a new framework for operating mobile

robots equipped with a laser scanning system in cluttered outdoor environments with the aid of a UAV. Chen et al. (2019) proposed a process using an imagery-based point cloud where a bridge inspection procedure was introduced, including data acquisition, 3D reconstruction, data quality evaluation, and subsequent damage detection.

Phillips and Narasimhan (2019) presented the challenges associated with automating data collection for the visual inspection of bridges, which were addressed using a ground-based robot and an autonomy framework. The developed inspection manager allows different sensors to be added to inspection plans by implementing the action client/server pair, and the navigation stratappliesable to the majority of UGVs, which can meet the requirements for management and execution of inspection plans. Elmekati et al. (2019) described the use of airborne Lidar in assessing the geotechnical health of the embankment supporting Chain O'Hills Road located in Woodbridge, NJ. The framework enables assessing existing conditions and predicting the future performance of these systems. Airborne Lidar technologies are effective in capturing data describing surface conditions for large-scale geotechnical systems.

Liu et al. (2021) proposed an augmented reality (AR) solution by integrating the UAV inspection workflow with a building information model (BIM). The method was based on designing an algorithm pipeline to drive the connective animation of the BIM and the aerial video.

2.4.2 Surveying

UAV uses in construction surveying have also been a popularly implemented category in the reviewed literature. Shang and Shen (2018) presented a pilot study using visual Simultaneous Localization and Mapping (SLAM) and UAVs for real-time construction site reconstruction. The

authors used the techniques in their methodology including earthwork measurement, construction progress management, and site asset tracking. Visual SLAM and UAVs were found to be more efficient tools for 3D reconstruction than photogrammetry on time-critical construction projects. Future studies should aim to overcome limitations with sensor fusion techniques and reactive UAV flight planning algorithms.

Asadi et al. (2020) designed a UAV-UGV system that integrated two custom-built mobile robots including one ground robot and one aerial blimp. A stereo camera and a Lidar sensor were used on the UGV for localization, autonomous navigation, and environment mapping. The UGV navigated toward pre-selected locations while being followed by the UAV using vision-based techniques. Jiang and Bai (2020) presented the results of using drone-based-orthoimages to estimate elevations. They found that the technique was effective in construction operations despite the possible distortion parameters and the contrast between the analyzed models. Jiang and Bai (2020) also evaluated the effectiveness of the Convolutional Neural Network (CNN) in site surveying and strengthened CNNs to work with large-scale construction site images. For further research, they suggested increasing the accuracy of the elevation estimation using image segmentation or image classification.

Jiang et al. (2020) proposed a method to obtain elevation from surfaces with ground vegetation which does not allow accurate orthoimages and CNNs. This study obtained accurate results identifying the obstacles regardless of the ground points with small elevation gaps on the joints. Jiang and Bai (2021) further proposed a method to determine construction site elevations using automatic and accurate drone-based low-high orthoimage pairs. Despite issues with the reflected rays, the image numbers and 3D reconstruction coverage were efficiently safe.

Martinez et al. (2021) investigated the single and dual frequency effects of post-processed kinematic (PPK) technology of the global navigation satellite system (GNSS) and its advantages in building surveying. The outcomes allowed the creation of a matrix that shows the accurate results of the techniques used. Future studies should also assess projects with larger surveying areas and conduct point cloud data accuracy assessment analyses based on RMSE calculations. Hou et al. (2021) studied how to utilize high-definition RGB images for more accurate tie-point detection, how different flight configurations affect tie-point data fusion, and how tie-point data fusion performance can be improved. The proposed tie point thermal and RGB data-fusion framework allowed for district-level thermal mapping to solve such problems. Further studies should choose a proper flight altitude that is higher than the highest building in the mapping area, and the selection of camera angles should be based on survey requirements.

2.4.3 Other Uses

Since few research studies were identified to focus on safety, monitoring, and training, they are summarized together here. Martinez et al. (2020) explored how UAV technology and their generated aerial visual contents might affect the current approach to conducting safety planning and monitoring on high-rise building construction sites in Chile. The case study provided the details of the new steps required in a high-rise building construction project to integrate UAVs and their generated visual data within the current safety planning and monitoring process. The main added steps were related to designing and conducting UAV flights and collecting and processing visual data.

Xiao et al. (2018) explored using a UAV to obtain videos of an excavation project to monitor slope stability at different stages of the operation. Based on the terrain points, the surfaces of interest were extracted, and their plane parameters were computed to estimate the

slope stability of the evolving excavation. This study demonstrated the feasibility of the proposed method and showed that a texture-rich 3D model of an excavation can be constructed from drone imagery and subsequently used for quantitatively evaluating slope stability and safety.

2.5 Summary

In recent years, there has been increased adoption of UAS use in various professional fields related to the construction industry. This phenomenon has been due to the technological advancements developed concerning UAS. Numerous individual research studies have been published regarding the use of UAS in construction projects; however, a summary of the findings of current research was needed. This research project spanned the years 2016-2021. A total of 95 papers from a list of 21 journals and conference proceedings were evaluated. This literature review generated the following conclusions:

- There has been a significant increase in the number of UAS research studies performed during the investigated timeframe;
- Worldwide, the United States leads in research related to the use of UAS for the field of construction management;
- Most UAS research related to construction has been focused on such topics as inspection, surveying, algorithms, and operations;
- RGB is the most common sensor type implemented in UAS research for construction; and
- The majority of the research using UAS for construction purposes has involved buildings, bridges, and roads.

CHAPTER 3 METHODOLOGY

3.1 Introduction

The flowchart depicted in Figure 7 presents the overall goal of this research. This section first presents the three primary objectives of this study. An extended overview of past research projects, concerning UAS uses for construction purposes in the timespan (2016-2021), is presented in the literature review section. This research involved several locations for data collection. These sites were selected based on the Federal Aviation Administration (FAA) PART 107 regulation entitled: “Small Unmanned Aircraft Systems.”

In this research project, two UAS were implemented. The DJI Matrice 300 RTK is a photogrammetric UAS system. Data collected with this UAS was then analyzed via DJI Terra and DroneDeploy software. The DJI Matrice 600 Pro is a customized LIDAR system. Autodesk ReCap Pro and Autodesk Civil 3D software were used to create the point cloud model based on the data from the DJI Matrice 600 Pro.

UAS flights were conducted, and data was collected concerning linear dimensions, field inspections, and volume calculations. The two sites for linear dimension measurements were the West Academic Building and shipping containers located on the ECU West Research Campus, Greenville, NC. There was a single site used for field inspection which was the Grimesland Bridge located in Pitt County, NC. Two sites were also used for volume calculation measurements. These sites were a treatment water building located on the West Research Campus, and an aggregate pile of bulk material located in the NCDOT Pitt County Maintenance Yard near the Pitt County Airport.

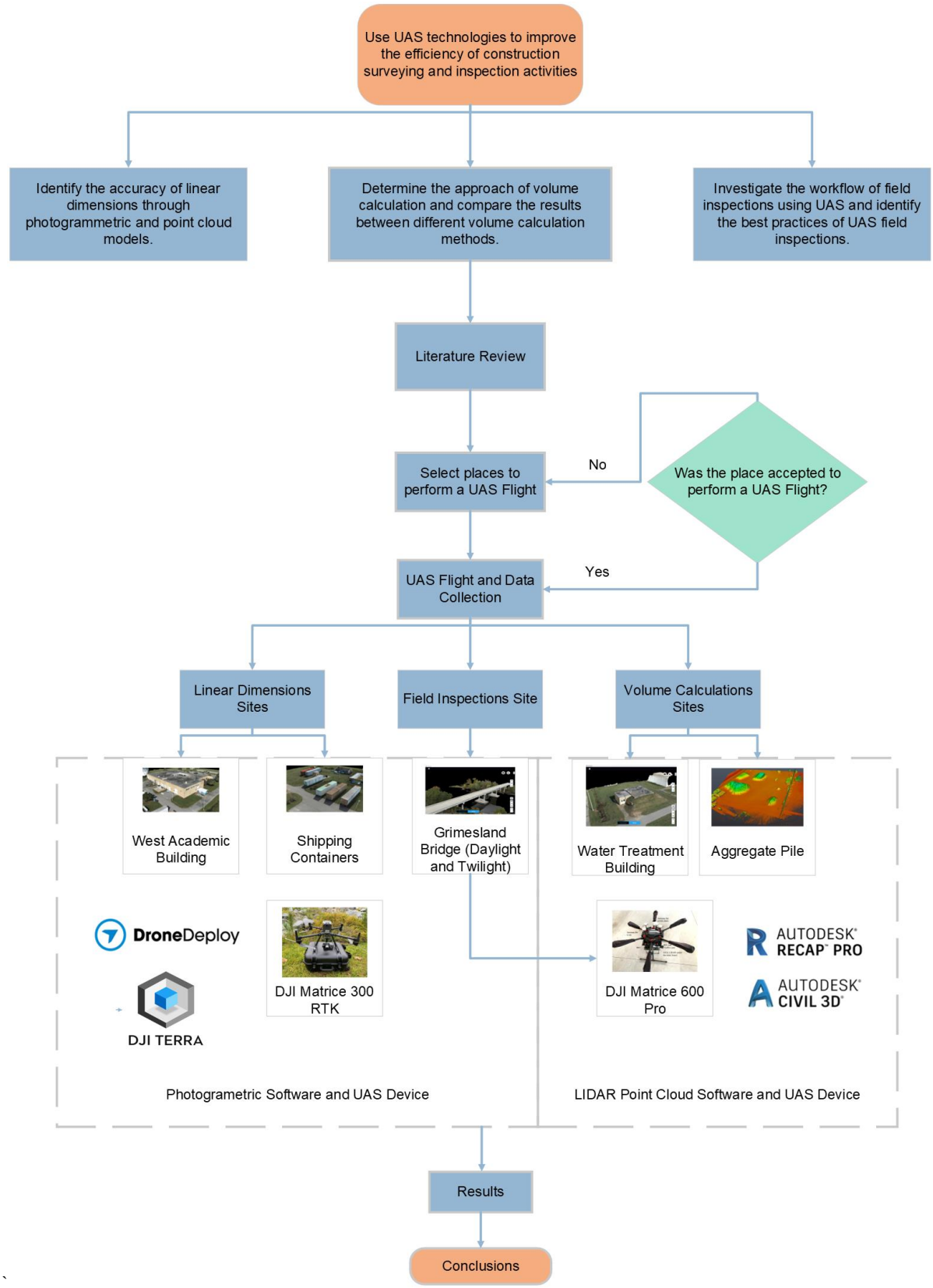

Figure 7. Flow Chart of Research Methodology

3.2 UAS Devices

3.2.1 DJI Matrice 300 RTK

A DJI Matrice 300 RTK commercial UAS was used for this research to create photogrammetric models. This UAS features 6-way directional sensors and provides a maximum of 55 minutes of flight time. The Matrice 300 UAS was equipped with a Zenmuse P1 full-frame image camera and paired with a DJI D-RTK 2 high-precision GNSS mobile station to provide the highest quality and accuracy of aerial images. This system can generate 2D maps and 3D photogrammetric models, as well as converted 3D point cloud models. The UAS and camera are depicted in Figure 8.

Figure 8. DJI Matrice 300 RTK

3.2.2 DJI Matrice 600 Pro

A customized DJI Matrice 600 Pro was used for this research to create LIDAR models. This UAS features a high payload capacity of 13.2 lb and a modular design to mount additional components. The Matrice 600 Pro was equipped with a SICK LD-MRS LIDAR sensor for

downward looking or a Velodyne PUCK-16 LIDAR sensor for side-view looking, and paired with a NovAtel OEM 6 GNSS base station to provide the highest quality and accuracy of LIDAR points. The customized components in the UAS-LIDAR System appear in Figure 9, including:

- An IDS uEye industrial image camera
- A GoPro Hero 5 video camera
- A SICK LD-MRS LIDAR sensor or a Velodyne PUCK-16 LIDAR sensor
- Three Raspberry Pi III-embedded computers
- A NovAtel SPAN GNSS-IMU with an antenna.

In addition, an error prediction model was developed to precisely calibrate the captured LIDAR points to achieve the desired accuracy, as detailed by Guan et al. (2022)

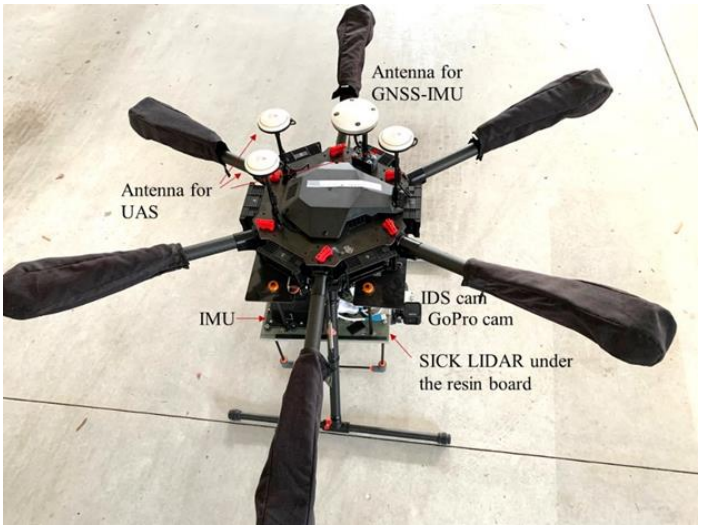

Figure 9. Components of DJI Matrice 600 Pro

3.3 Software

3.3.1 DJI Terra

DJI Terra is an all-in-one drone mapping solution which allows for the analysis of aerial data. This 3D modeling and mapping software converts drone data into digital features for easy analysis and decision-making. The software has real-time mapping capabilities, in order to assess vehicle crashes, track progress on construction projects, or conduct large-scale critical infrastructure inspections on bridges and roadways. It is a useful surveying tool for the collection of data such as area, distance, and waypoints. Figure 10 illustrates an example of the view using this software.

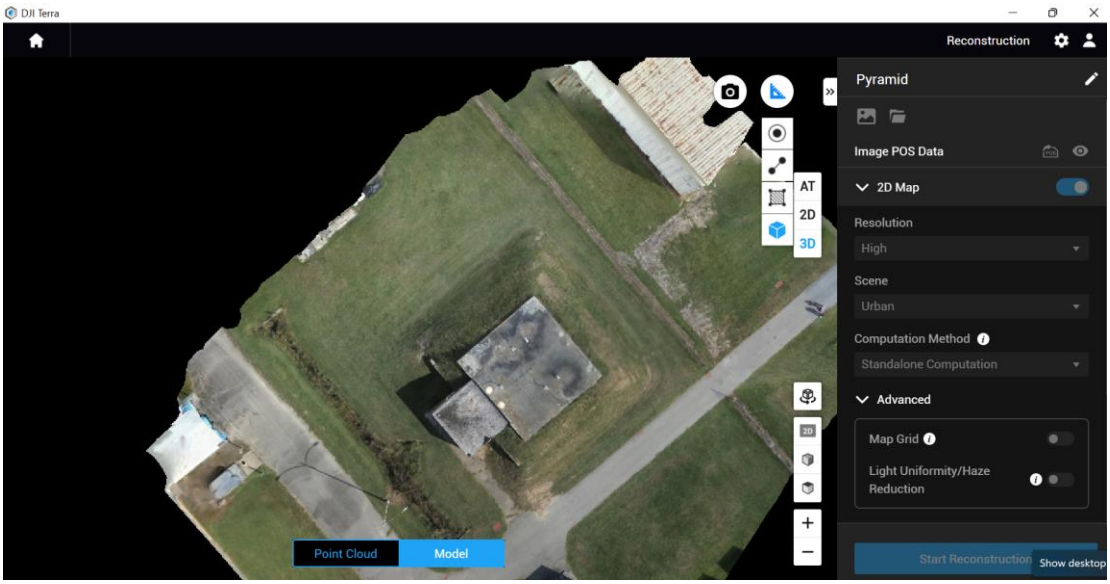

Figure 10. DJI Terra Software Window View

3.3.2 Drone Deploy

DroneDeploy is an easy and fast application for creating aerial maps and 3D models. This software allows the creation of 2D maps, digital elevation models, and 3D models. It contains

features such as annotations, volumetric analysis, and Normalized Difference Vegetation Index (NDVI) analysis. An example of a DroneDeploy window view is presented in Figure 11.

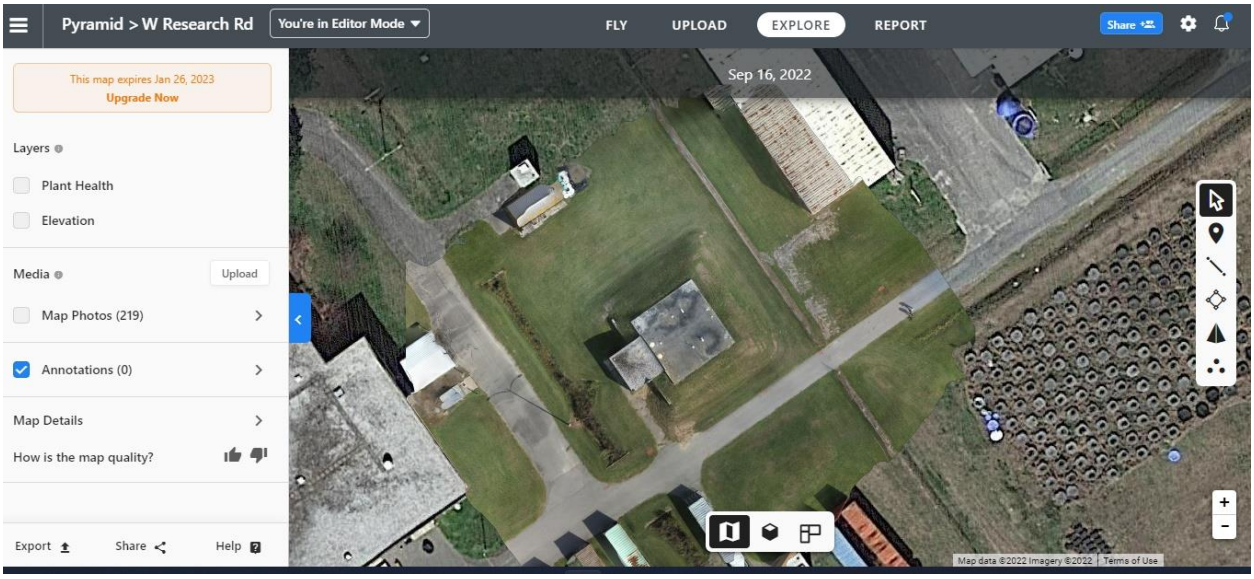

Figure 11.DroneDeploy Software Window View

3.3.3 Autodesk ReCap Pro

As shown in the example of the window view presented in Figure 12, Autodesk ReCap Pro is a 3D program utilized for laser scanning and photogrammetry projects. It exports files into other Autodesk software applications. Autodesk ReCap Pro is useful for importing, exporting, and assimilating UAS project data. It provides a process to transform photogrammetric and point cloud data into 2D and 3D models.

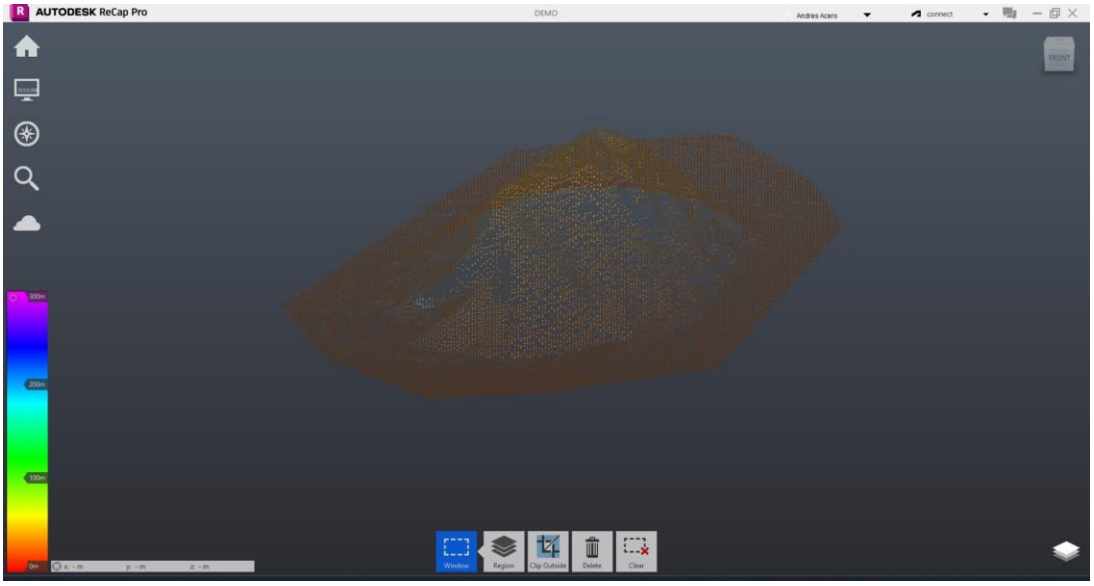

Figure 12.Autodesk ReCap Pro Software Window View

3.3.4 Autodesk Civil 3D

Autodesk Civil 3D is a type of engineering software that is used for multiple construction surveying and design projects such as road construction, and for water, sanitary and storm sewer analysis. Its dynamic feature provides consistent construction documentation, which remains synchronized even as design changes are made to the model. An example of an Autodesk Civil 3D window view is presented in Figure 13.

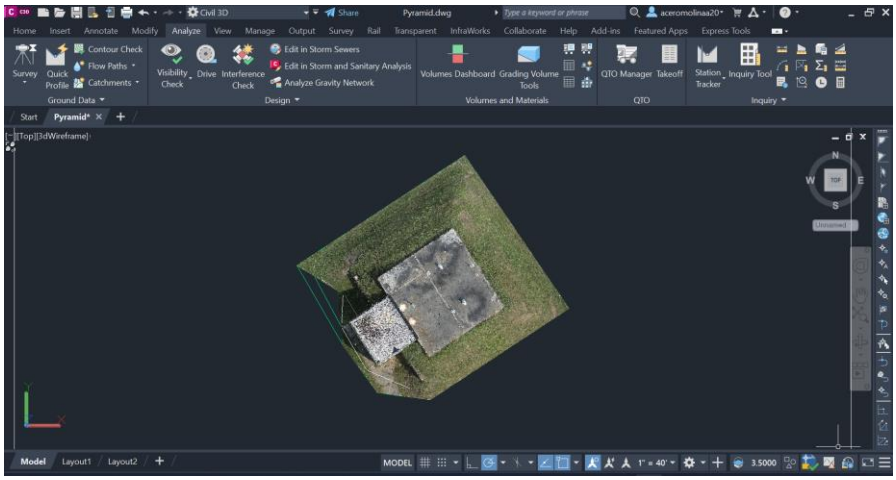

Figure 13.Autodesk Civil 3D Software Window View

3.4 Field Testing

Table 3 introduces the flights scheduled for this research project. In order to perform the UAS flights, permission was necessary from different organizations following the regulations specified in Part 107 of the FAA.

Table 3 Summary of the Performed Flights

Flight	Date	Altitude (ft AGL)	Area (m^2)	Photos	UAS
West Academic Building	09/02/2022	250	6811	162	M300 RTK
Containers	09/16/2022	80	1755	527	M300 RTK
Water Treatment Building	09/16/2022	80	778	219	M300 RTK
Aggregate pile	03/22/2022	30	-	LIDAR	M600 Pro
Grimesland Bridge	03/22/2022	30	-	LIDAR	M600 Pro
Grimesland Bridge	10/14/2022	220	10759	357	M300 RTK
Grimesland Bridge (Twilight conditions)	02/03/2023	220	10759	357	M300 RTK

3.4.1 ECU West Academic Building

The ECU West Research Campus houses the West Academic Building. The campus covers almost 600 acres northwest of Greenville, NC. It has an environmental health onsite wastewater demonstration facility. Its location provides a great advantage when performing UAS flights because it is in a rural area, free of possible obstacles and hazardous objects such as cables, people, and traffic. This site was chosen as the testing area to verify the features and effectiveness of the DJI Matrice 300 RTK commercial UAS system. Additionally, other West Research Campus sites were used to obtain test measurements of distances and volumes. Figure 14 presents a view of the West Research Campus, retrieved from Google Earth (Google 2022), and Figure 15 illustrates the West Academic Main Building. This building's architectural plans

were obtained to verify different measures shown in the plans drawn by the Austin Company in the 1960s. It was not possible to find an updated version of the architectural design for this building.

Figure 14. ECU West Research Campus

Figure 15. West Academic Main Building

On September 2, 2022, UAS test flights were performed in order to verify the features and effectiveness of the DJI Matrice 300 RTK commercial UAS system This research involved a total of 162 photos. The area covered was 6811m^2, and the distance that the UAS flew was 5423 ft. The altitude above the ground level was 250 ft. The Zenmuse P1 camera utilized a Smart Oblique Capture to obtain images at different oblique angles for photogrammetric model generation. Flight plan details concerning distance, estimated time, waypoints, photos, and mapping area are represented in Figure 16, for the West Academic Building.

Figure 16. UAS Flight Plan for the West Academic Building

3.4.2 Shipping Containers

These structures are located within the ECU West Academic Research Campus. Their heights are identical, and their characteristics are described in Chapter 4, Section 4.3. A photo of the containers taken onsite is shown in Figure 17.

Figure 17. Shipping Containers

A 3D view of the shipping containers was obtained using DJI Terra and is illustrated in Figure 18. Five of the six are labeled as 40 ft Dry containers (1, 2, 3, 4, and 6) and have the same fabrication features. The other (5) is a 45 ft Dry container.

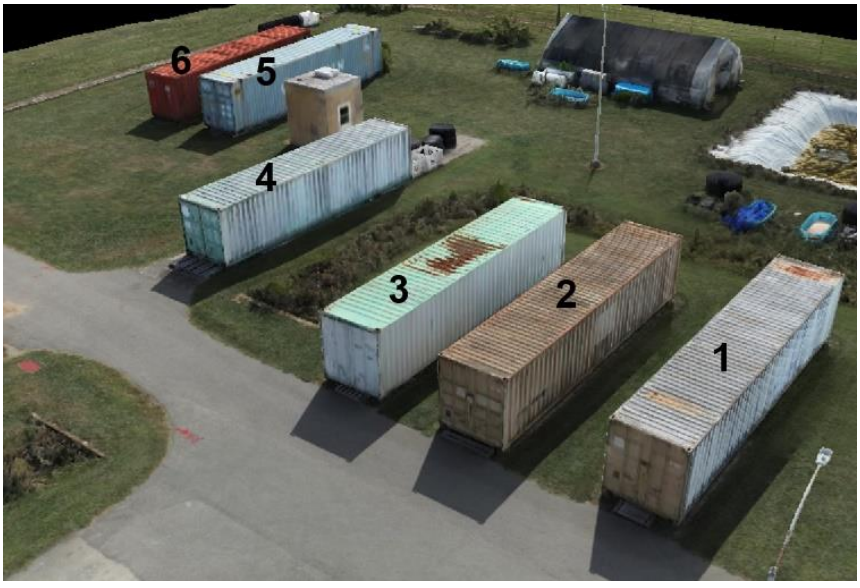

Figure 18. 3D Model of the Shipping Containers

This flight was performed on September 16, 2022. A total of 527 photos were taken. The area covered was 1755 m^2; 3825 ft was the distance that the UAS flew; and 80 ft above the ground level was the attitude. A Smart Oblique Capture was used with the Zenmuse P1 camera to obtain images at different oblique angles for photogrammetric model generation. General details of the performed flight are represented in Figure 19 indicating distance, estimated time, waypoints, photos, and mapping area.

Figure 19 UAS Flight Plan for the Shipping Containers

3.4.3 West Water Treatment Building (WWTB)

The West Water Treatment Building (WWTB) is also located on the West Research Campus. It is an underground concrete tank with a machine room. This building was chosen for this research because its geometry and levels allowed for the assessment of volume values. A ground slope surrounds this structure as demonstrated in Figure 20.

Figure 20. West Water Treatment Building

Figure 21 presents a 3D model of the WWTB obtained using DJI Terra.

Figure 21.3D Model of the West Water Treatment Building

The flight to obtain the volume measurements for the WWTB was performed on September 16, 2022, and a total of 219 photos were taken. The area covered was 778m^2. The distance that the UAS flew was 2831 ft, at an altitude of 80 ft above ground level. The Smart Oblique Capture was used with the Zenmuse P1 camera to obtain images at different oblique angles for photogrammetric model generation. The performed flight yielded distance, estimated time, waypoints, photos, and mapping area data, and the flight plan is illustrated in Figure 22.

Figure 22. UAS Flight Plan for the West Water Treatment Building

3.4.4 Aggregate Pile

The North Carolina Department of Transportation (NCDOT) Pitt County Maintenance Yard is located near the Pitt County Airport. The area of interest for this research is approximately 80m by 160m. There are several piles composed of different materials in this maintenance yard, and a single pile was chosen for this study. As requested by the airport, the UAS flight at this location was kept at a low altitude (<60 ft above ground). The flight lasted 15

minutes and was performed manually, although the customized DJI Matrice 600 Pro only needed 5 minutes to scan all the piles. The location of the aggregate pile is indicated, in Figure 23, by a red circle.

Figure 23. Location of the Aggregate Pile within the Pitt County Maintenance Yard

The Matrice 600 Pro flight was performed on March 22, 2022. The captured LIDAR point cloud was processed with the developed error prediction model, as described by Guan et al. (2022). The accuracy of the determined values was approximately 0.1m for random errors and centimeter-level systematic errors.

3.4.5 Grimesland Road Bridge

The UAS measurement flights were performed at the L. Elmore Hodges Bridge, completed in 2011 and located in the town of Grimesland, NC. It spans the Tar River with a

width of approximately 308 ft, measured between the piers located on each side of the river. Figure 24 shows a view of the Grimesland Bridge.

The bridge is a typical beam bridge that consists of horizontal beams supported at each end by piers. A total of 19 bents supports the bridge deck and the designed live loads (vehicular traffic) over 20 spans, for a total length of 1963.25 ft. The bridge has a rip rap located at the beginning of bent 1, which is composed of limestone or granite chunks that have been quarry-cut. A typical fractured face is at least 12-18 inches long and has at least two fractured surfaces, with the rocks positioned next to one another. Structural plans for the Grimesland Bridge were obtained from the North Carolina Department of Transportation to verify multiple measurements of the spans, sections, piers, and foundations.

Figure 24. View of the Grimesland Bridge

For this research, a Matrice 300 RTK flight in daylight conditions was performed on October 14, 2022, with an automatic flight mission. A total of 357 photos were taken during the

10-minute flight, covering 14.4 acres of area with an accuracy of camera GPS location at 0.03 ft, 0.04 ft, and 0.04 ft in the X, Y, and Z directions, respectively. The flight altitude was maintained at 220 ft above ground level to avoid surrounding trees. Smart Oblique Capture was used with the Zenmuse P1 camera to capture images at different oblique angles for photogrammetric model generation. Figure 25 presents an onsite screenshot of the UAS's remote control which shows the automatic flight route, estimated distance, flight duration, number of photos, and the mapping area. The actual results varied slightly from the estimated values. Another flight using the Matrice 300 RTK was performed in twilight conditions on February 3, 2023. This flight had the same characteristics as the flight performed in daylight conditions.

Figure 25. UAS Flight Plan for the Grimesland Bridge

The Matrice 600 Pro flight was performed separately on March 22, 2022. The UAS was manually operated at a low altitude over the bridge during the 5-minute flight. The error prediction model was developed using the captured LIDAR point cloud data, as described by Guan et al. (2022a). The accuracy of the results involved an error value of 0.1m.

CHAPTER 4 VERIFICATION OF LINEAR DIMENSIONS

4.1 Introduction

Linear dimensions from different structures were verified using the DJI Matrice 300 RTK commercial UAS system which involved the following sources: building plans and the datasheet for the specified structure. These measurements provided a means to test the accuracy of UAS commercial system measurements. The values obtained from photogrammetric and extracted point cloud models using DJI Terra comprise the comparison data presented in this chapter, for the West Academic Building and the six shipping containers.

4.2 West Academic Building

For the West Academic Building, architectural plans were obtained to compare the different measurements from these blueprints with the measurements obtained through the UAS flights. The results of these comparisons were recorded as a percentage of error. The building plan obtained to verify the measurements for the West Academic Building is shown in Figure 26.

This architectural plan was designed by hand and includes the entire architectural information in a single drawing sheet. It presents the measurements using building's section to specify the location of each side of the structure. In addition, the plan labeled the linear measurements of all the sections. Therefore, the verification of the linear measurements of these side in comparison with the data obtained using the UAS is annotated as mentioned in Table 4.

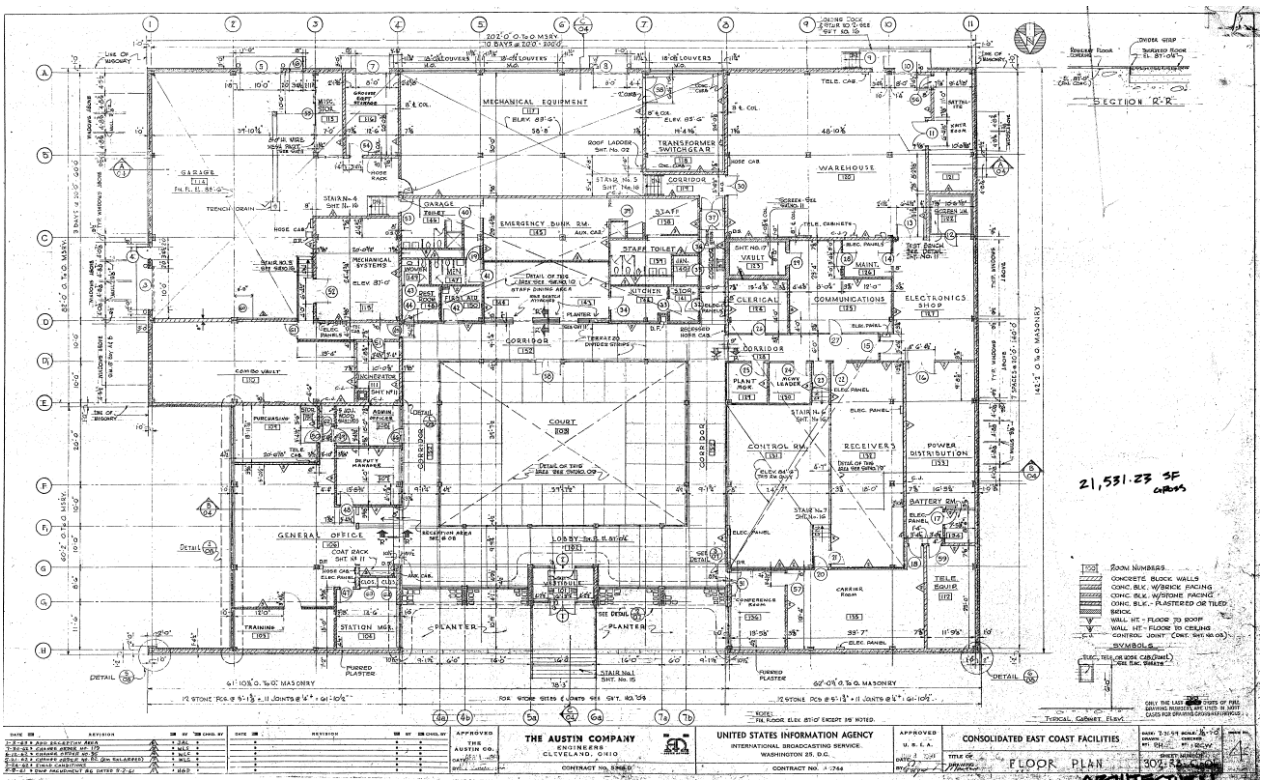

Figure 26. West Academic Center Building Plan

Table 4 illustrates the measurements obtained from the plan and summarizes all the data obtained for the different UAS systems.

Table 4. Data from the West Academic Building and the UAS System Measurements

	Linear Dimensions (ft)						
Location / Method	**N(1-4)**	**N(4-8)**	**N(8-11)**	**E(A-E)**	**E(E-H)**	**S**	**W**
Plan	61.88	78.25	62.04	82.00	60.17	202.00	142.17
DJI 2D	61.42	78.18	61.98	82.09	60.17	201.97	142.09
Terra 3D	61.78	78.18	62.01	82.09	60.14	202.20	142.19
Drone Deploy	61.84	78.21	62.00	81.96	60.13	201.96	142.13
Autodesk Civil 3D	61.75	78.15	61.98	82.06	60.11	202.17	142.16

The highest difference was calculated for one of the sides of the West Academic Building (North between gridlines 1-4) using the DJI Terra 2D view. This result indicates a variation of

0.46 ft between the value obtained using the photogrammetric model (61.42 ft) and the design value (61.88 ft).

4.3 Shipping Containers

Table 5 contains the data for the containers labeled 1,2,3,4, and 6. Table 6 contains the data for the container labeled 5. The 3D view of all of the containers is presented in Chapter 3, Figure 18. Both Table 5 and Table 6 introduce the data obtained from the different linear measurements for the containers located on the West Academic Research Campus. As demonstrated in Figure 27, all the containers have their datasheet (Solutions 2016). Five of the six are labeled as 40 ft Dry containers having the same fabrication features. The other is a 45 ft Dry container. According to the datasheet for each container, all of them have standard measurements.

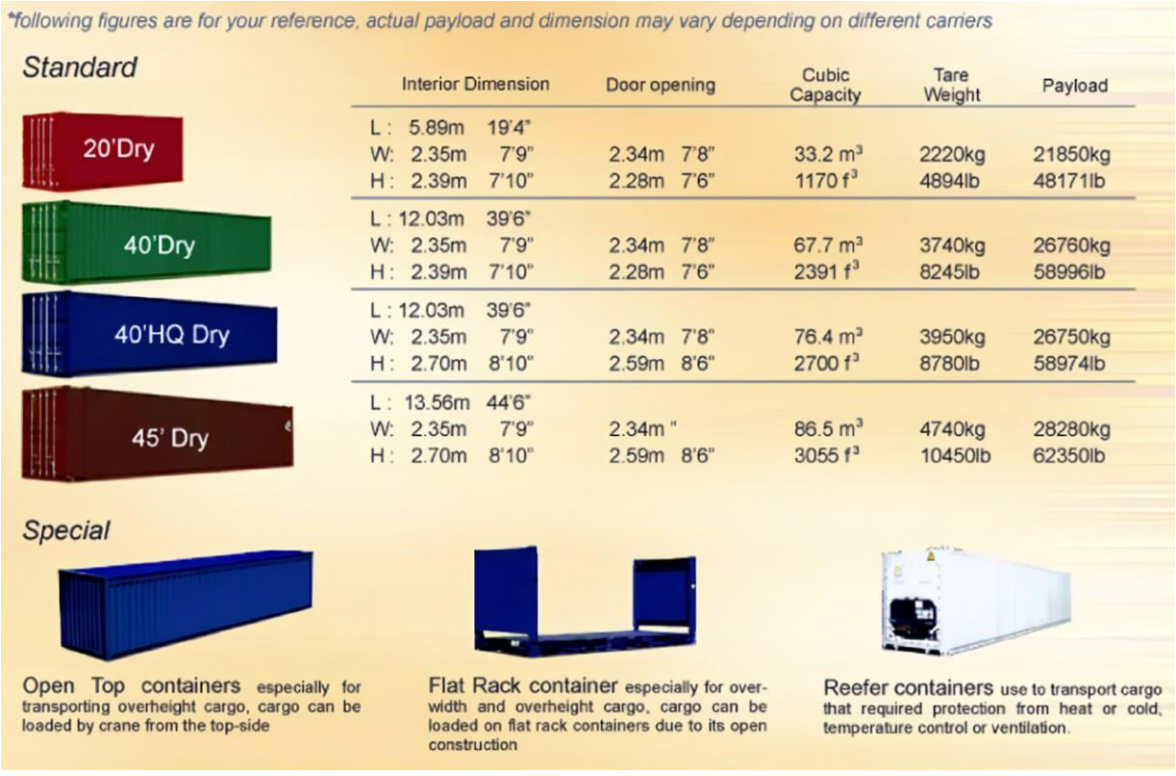

Figure 27. Shipping Container Specifications

According to the values obtained, the higher variations appear in all of the height measurements for the containers listed in Table 5 and Table 6. In reference to the factory data, the highest percentage of error was obtained using DJI Terra. Values obtained regarding length and width measurements demonstrated more accuracy in comparison with the datasheet for each shipping container.

Table 5. Data Obtained from the Shipping Containers 40' Dry Type

Method \ Dimension		Length (ft)	Width (ft)	Height (ft)
Factory Data		40.00	8.00	9.50
DJI Terra	2D	39.90	7.94	9.20
	3D	39.90	7.94	9.10
Drone Deploy		39.90	7.94	9.25
Autodesk Civil 3D		39.70	7.95	9.24

Table 6. Data Obtained from Shipping Container 45' Dry Type

Method \ Dimension		Length (ft)	Width (ft)	Height (ft)
Factory Data		45.00	8.00	8.50
DJI Terra	2D	44.88	7.91	8.38
	3D	44.88	7.91	8.40
Drone Deploy		44.88	7.91	8.42
Autodesk Civil 3D		45.00	7.95	8.34

The highest variations for all of the measurements are associated with the height values for both types of containers. The variations are within the range of 0.08 ft and 0.16 ft.

4.4 Summary

Linear measurements were calculated for the purpose of verifying the features and performance of the DJI Matrice 300 RTK commercial UAS system, prior to field inspection of the Grimesland Bridge. The site chosen for this research purpose was the ECU West Research

Campus in Greenville, NC. Measurements were obtained for the West Academic Building and six shipping containers located at this site. The data collected using the commercial UAS system was compared with the architectural plan for the West Academic Building and the datasheet for each container.

The highest variation for linear calculations of the West Academic Building was -0.74% using DJI Terra 2D, which represents 0.45 ft for the N (1-4) side. This side has a length of 61.88 ft based on the design plans. The highest variations for the shipping containers were present for the height values, these values are in the range of 0.08 ft and 0.16 ft.

CHAPTER 5 COMPARISON OF VOLUME CALCULATIONS

5.1 Introduction

For the aggregate pile located in the NCDOT maintenance yard, the volume comparison was performed using 3 different types of data (GPS points, extracted LIDAR points, and full point cloud), as a means to determine the differences between conventional surveying data and data obtained using a customized DJI Matrice 600 Pro UAS system.

The West Water Treatment Building was selected as the site for volume calculation comparisons using the DJI Matrice 300 RTK commercial UAS system. The building is a structure located within the ECU West Research Campus. It has a regular trapezoidal figure with slopes on each side, to stabilize the walls of the water tank that is embedded half underground. Photogrammetric models were obtained for this structure in order to calculate volume differences using DJI Terra and DroneDeploy. In addition, an extracted point cloud using DJI Terra was obtained to assess the volume via Autodesk Civil 3D.

The comparison between the volume values obtained using the traditional surveying methods and the values for a customized UAS system is presented in Chapter 5, Section 5.2. The results of the volume calculations, for the data obtained through the UAS commercial system which created volume models using different photogrammetric and point cloud software, are presented in Section 5.3.

5.2 Aggregate Pile

5.2.1 Volume from GPS Surveying Points

At the NCDOT site, the device used to obtain surveying information was a Bentley MicroStation V8i, which generates a Triangulated Irregular Network (TIN) for volume

calculations. Since MicroStation V8i has been phased out and no longer available, Autodesk Civil 3D was utilized to replicate the results for comparing traditional surveying with data obtained using a customized LIDAR UAS system. The 36 coordinate points measured via surveying GPS were imported into Autodesk Civil 3D. Then, a base surface was created from the perimeter points assuming the bulk pile sits on an even and flat surface, and a slope surface was created from all points, as shown in Figure 28. The numbers on the base surface represent the elevations of the perimeter points in feet. The elevations of the slope surface points were in the range between 38 ft to 41ft.

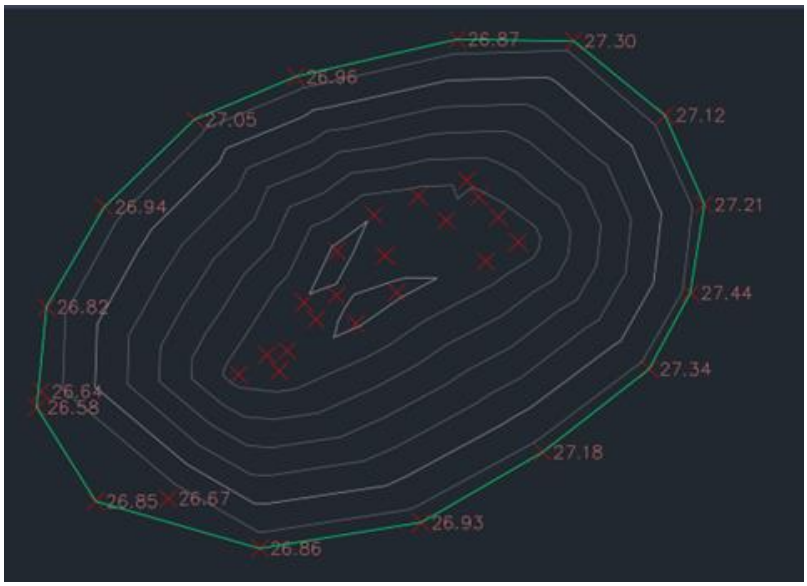

Figure 28. Base and Slope Surfaces of Surveying GPS Points in Autodesk Civil 3D

Figure 29 presents a comparison between the 3D volume models generated by MicroStation V8i and Autodesk Civil 3D, respectively, based on the assumption of the base surface being an even and flat surface. The transparent volume model in Figure 29(a) shows a total volume of 351.53 cubic yards based on data from MicroStation V8i. The solid volume model in Figure 29(b) was generated in Autodesk Civil 3D, which calculated the volume between the base surface and the slope surface.

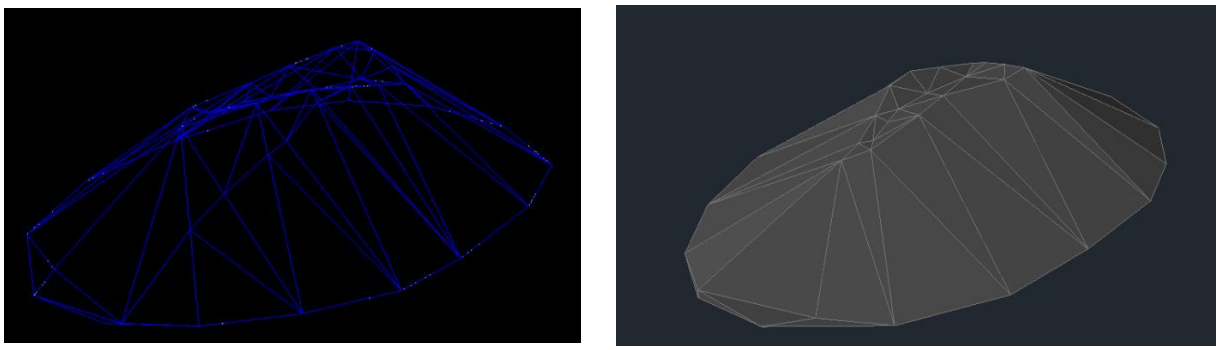

(a) Volume Model in MicroStation (b) Volume Model in Autodesk Civil 3D

Figure 29. 3D Volume Models from Surveying GPS Points

As demonstrated in Figure 30, the calculated volume is shown in the Net(adjusted) column. This is the volume analysis result obtained from Autodesk Civil 3D.

Fill Factor	Cut Factor	Style	2d Area(Sq. Ft.)	Cut(adjusted)(Cu. Yd.)	Fill(adjusted)(Cu. Yd.)	Net(adjusted)(Cu. Y...	Net Graph
1.000	1.000	_No Display	1650.87	0.00	351.53	351.53<Fill>	

Figure 30. Calculated Volume from Surveying GPS Points in Autodesk Civil 3D

5.2.2 Volume from Extracted LIDAR Points

A developed algorithm was applied to extract the closest matches for the 36 surveying GPS points from the full point cloud, based on their coordinates which had slightly different elevations than the surveying GPS points. The 36 extracted points were then determined following the same process as in Autodesk Civil 3D to create the same base surface and a slope surface. Next, a 3D model was generated to calculate the volume between the two surfaces. Figure 31 illustrates the two surfaces and volume model of the aggregate pile, using extracted LIDAR points in Autodesk Civil 3D.

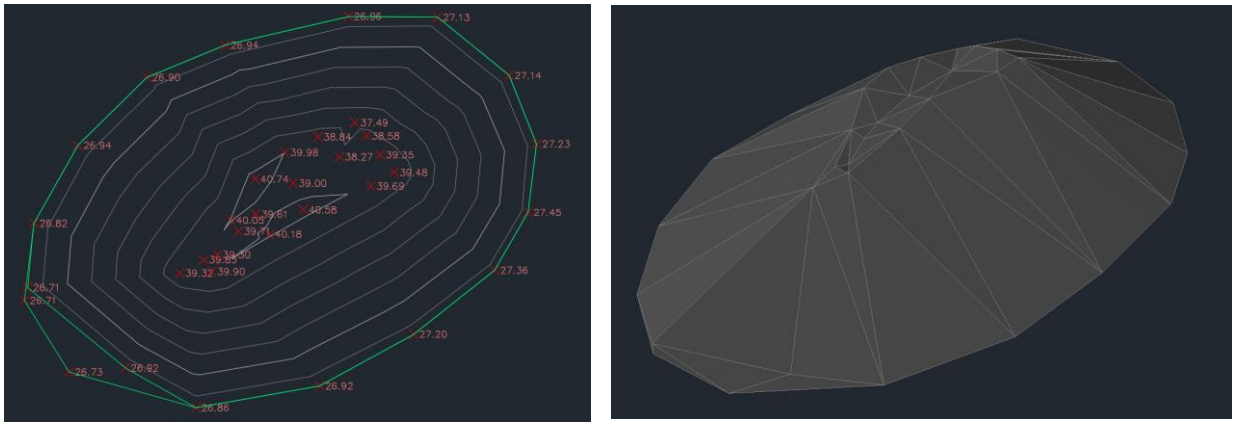

(a) Base Surface and Slope Surface (b) 3D Volume Model

Figure 31. 3D Volume Models from Extracted LIDAR Points

The same process as used for GPS volume calculation was implemented to calculate the volume of the aggregate pile, from extracted LIDAR points in Autodesk Civil 3D. The result was 354.84 cubic yards as presented in the Net(adjusted) column in Figure 32. This outcome was less than 1% larger than the volume calculated from the surveying GPS points, which is considered to be negligible in bulk material volume measurements.

Fill Factor	Cut Factor	Style	2d Area(Sq. Ft.)	Cut(adjusted)(Cu. Yd.)	Fill(adjusted)(Cu. Yd.)	Net(adjusted)(Cu. Y...	Net Graph
1.000	1.000	_No Display	1607.21	0.00	354.84	354.84<Fill>	

Figure 32. Calculated Volume from Extracted LIDAR Points in Autodesk Civil 3D

5.2.3 Volume from Full Point Cloud

Finally, the full point cloud obtained using the customized UAS LIDAR system for the entire maintenance yard was processed in Autodesk ReCap Pro. After the removal of the points outside of the aggregate pile to be measured, as circled in Figure 33(a), approximately one million points remained.

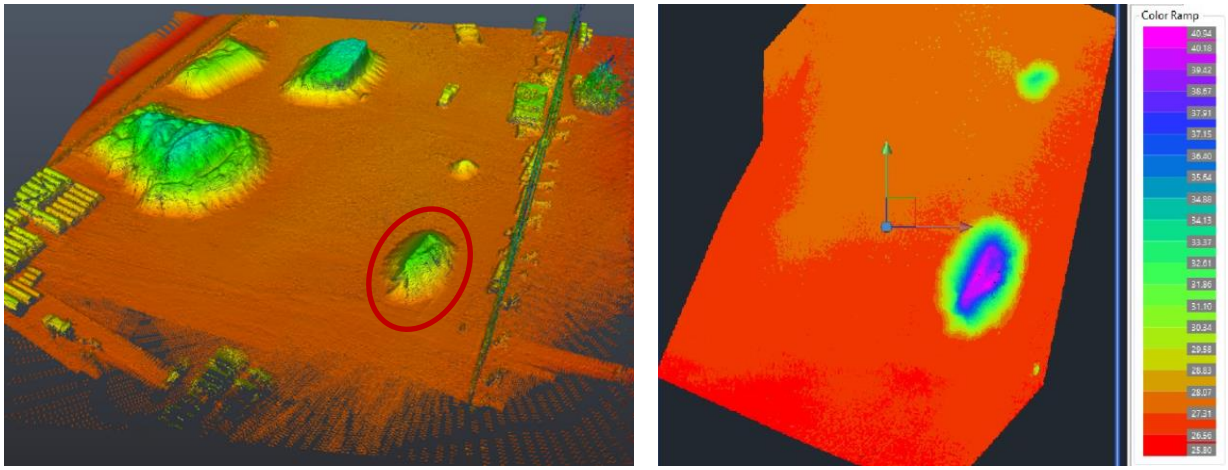

(a) Full Point Cloud in Autodesk ReCap Pro

(b) Elevation Spectrum Map in Autodesk Civil 3D

Figure 33. Full Point Cloud of the Maintenance Yard

The cropped point cloud was then imported to Autodesk Civil 3D following the same procedures as demonstrated in Figure 34. Since the base surface and the slope surface were now connected, it was necessary to identify the elevation of the base surface being used earlier and separate it from the slope surface. A detailed elevation spectrum map was created in Autodesk Civil 3D, with elevation intervals at 0.76 ft, to determine the cutoff elevation between the two surfaces. A cutoff elevation value of 27.10 ft was selected after carefully examining the elevation spectrum map, as shown in Figure 33(b).

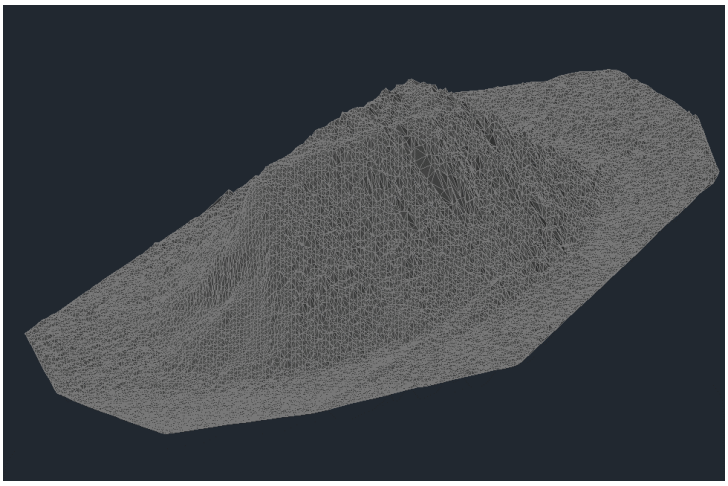

Figure 34. Volume Model of Full LIDAR Point Cloud in Autodesk Civil 3D

After separating the slope surface from the base surface, similar procedures were followed to calculate the volume of the bulk pile from the full LIDAR point cloud. Figure 35 shows the value in the Net(adjusted) column as 292.39 cubic yards, which was approximately 17% smaller than the surveying GPS point method as well as the extracted LIDAR point method.

Fill Factor	Cut Factor	Style	2d Area(Sq. Ft.)	Cut(adjusted)(Cu. Yd.)	Fill(adjusted)(Cu. Yd.)	Net(adjusted)(Cu. Y...	Net Graph
1.000	1.000	_No Display	3344.85	0.08	292.39	292.32<Fill>	

Figure 35. Calculated Volume from Full LIDAR Point Cloud in Autodesk Civil 3D

5.3 West Water Treatment Building (WWTB)

For this structure, different volume measurements were obtained using photogrammetric and point cloud software. Figure 36 shows the model obtained using DJI Terra. The area covered is indicated in red, and the points depicting the limits of the structure are illustrated. The volume value is calculated in cubic feet.

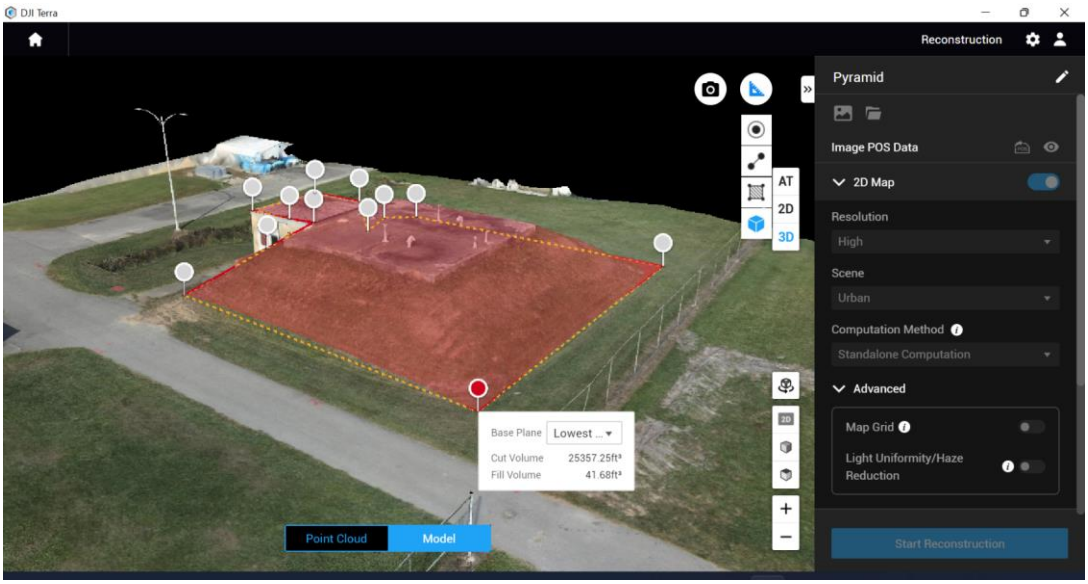

Figure 36. Volume of WWTB obtained from DJI Terra

The model obtained using DroneDeploy is presented in Figure 37. This model shows an isometric view of the area covered, which is indicated in blue. This volume value is expressed in cubic yards.

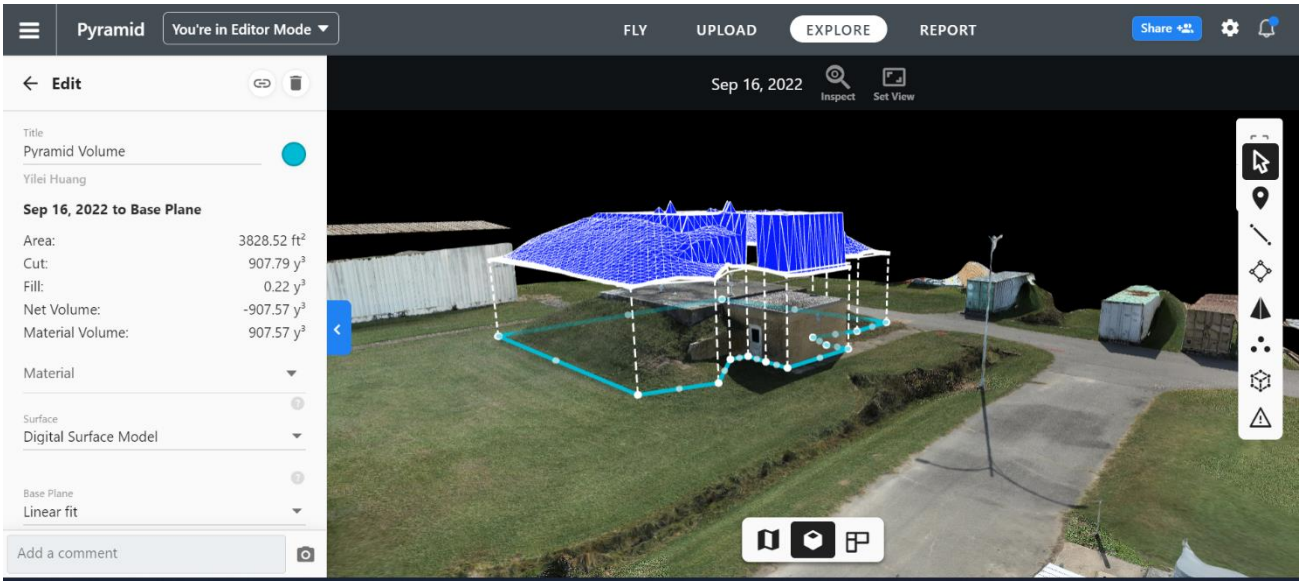

Figure 37. Volume of WWTB obtained from DroneDeploy

Volume measurements were determined using extracted point cloud data obtained with DJI Terra, in order to generate a 3D model based on Autodesk Civil 3D, as shown in Figure 38.

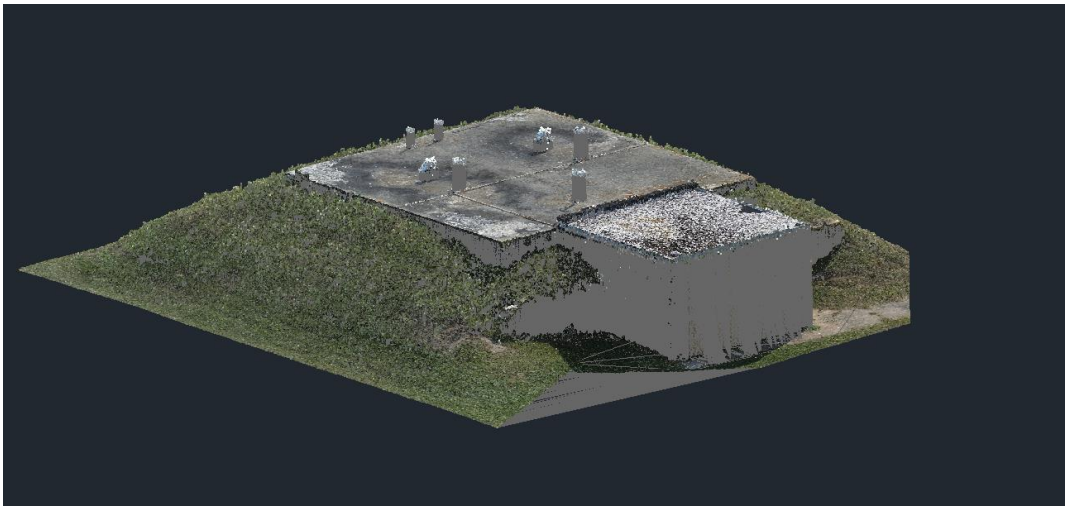

Figure 38. Model of the WWTB obtained from Autodesk Civil 3D

The volume value using the model obtained with Autodesk Civil 3D is introduced in Figure 39, in the Net(adjusted) column. The volume obtained was 871.17 cubic yards.

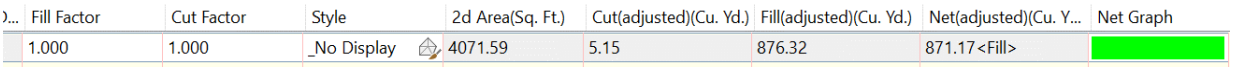

)...	Fill Factor	Cut Factor	Style	2d Area(Sq. Ft.)	Cut(adjusted)(Cu. Yd.)	Fill(adjusted)(Cu. Yd.)	Net(adjusted)(Cu. Y...	Net Graph
	1.000	1.000	_No Display	4071.59	5.15	876.32	871.17<Fill>	

Figure 39. Calculated Volume from the Point Cloud Model for the WWTB

Table 7 summarizes the results of volume measurements of the WWTB obtained using photogrammetric and point cloud software.

Table 7. Comparison of Volume Measurements of WWTB

Model	Software	Volume Total (cubic ft)	Volume Total (cubic yd)
Photogrammetry	DJI Terra	25357	939.15
	DroneDeploy	-	907.79
Point Cloud	Autodesk Civil 3D	-	871.17

The values in Table 7 were calculated using randomly selected points for each model.

5.4 Summary

For volume calculations, this study compared the data obtained using traditional surveying methods with data from a customized DJI Matrice 600 Pro UAS system that was equipped with a LIDAR sensor. An aggregate pile located close to Pitt-Greenville Airport, and situated in a maintenance yard belonging to the NCDOT, was selected for determining volume measurements using three different types of data: GPS points; extracted point cloud; and full point cloud. The first data type was determined via a MicroStation Vi8 system. The last two data types were obtained from the customized UAS system. The extracted point cloud file matched the same coordinates as the GPS point file, with slight differences in elevations. Using Autodesk Civil 3D and Autodesk ReCap Pro, the three different models for each data type were created.

The GPS points and the extracted point models showed similar volume values. The full point cloud model yielded a volume value that is approximately 17% less, in comparison with the other models. This difference was likely due to the full point cloud model involving more data than the other models. The models obtained using GPS and extracted point cloud data presented geometrical shapes having inaccurate surface slopes; consequently, these volume values could have overestimated the real surface. However, since the true base surface is unmeasurable and can even change under the weight of the pile, the true volume and accuracy cannot be determined and only the volume differences between the three measurement methods can be observed (Guan et al., 2022b).

The DJI Matrice 300 RTK commercial UAS system was used to obtain volume calculations for the West Water Treatment Building located on the ECU West Research Campus. This structure was chosen because its geometry allows for the calculation of the volume of the entire structure. The obtained data were analyzed using photogrammetry software (DJI Terra and DroneDeploy) and point cloud software (Autodesk ReCap Pro and Autodesk Civil 3D).

CHAPTER 6 INSPECTION OF BRIDGE STRUCTURES

6.1 Introduction

Present-day field inspections require significant labor, costs, and time. For these reasons, construction projects require innovative new techniques to obtain onsite information for such purposes as validation, verification, and assessment of the general status of structures. Therefore, the customized DJI Matrice 600 Pro system was utilized for one flight in order to obtain a full point cloud model, and the DJI Matrice 300 RTK commercial UAS system performed 2 flights as a means to obtain photogrammetric models in daylight and twilight conditions.

The models obtained from this data were used to measure different sections and dimensions represented in the structural design plans for the Grimesland Bridge. As an example, both Spans A, B, and C were measured and verified, and general details of the Rip Rap System located at the beginning of the bridge were identified, for the information depicted in Figure 40.

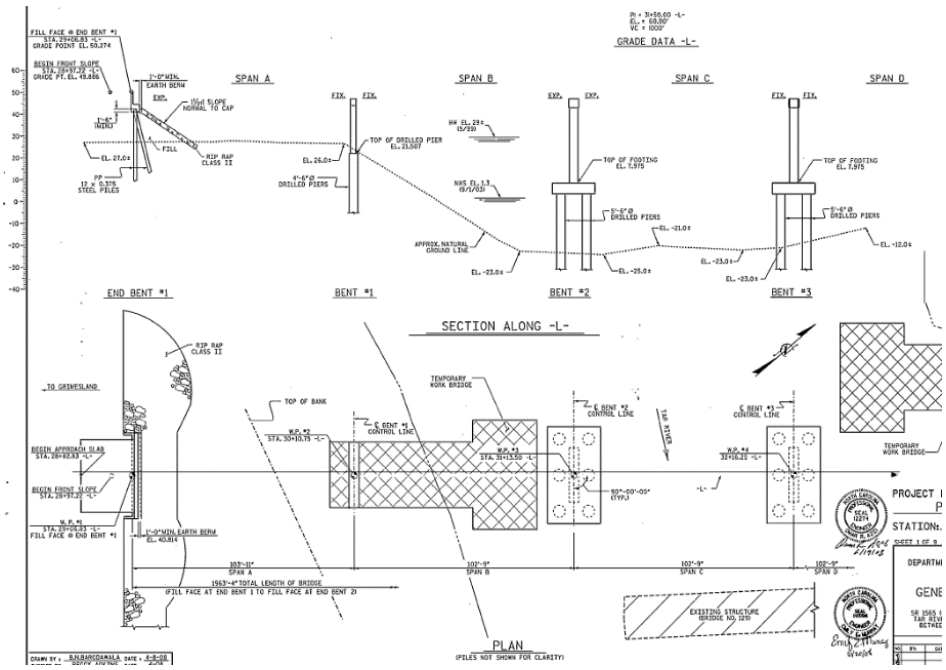

Figure 40. Longitudinal Section of the Bridge from Span A to Span D

6.2 Field Inspection Results

The results of the comparison between the structural design plans and the data obtained are presented in this chapter, as well as the models and percentages of error. Sections 6.2.1 and 6.2.2 only illustrate models obtained from DJI Terra. However, the results presented in Table 8 and Table 9 include the measurements obtained using both photogrammetric software: DJI Terra and DroneDeploy.

6.2.1 Photogrammetric Model in Good Light Conditions

Figure 41 demonstrates a daylight view of the 3D photogrammetric model in DJI Terra for the Grimesland Bridge which illustrates the full details of the bridge deck, spans, piers, and foundations. Linear dimensions were obtained in both the 3D model and the 2D map view, using horizontal distances as a length or width dimension.

Figure 41. Daylight Photogrammetric Model of the Grimesland Bridge in DJI Terra

Table 8 presents the comparison of the linear dimensions of three spans, a footing, and a deck section from DJI Terra and DroneDeploy, respectively, with the design values from the

structural plans. The variation of the measurements obtained from the photogrammetric models were compared with the data from the design plans. The greatest variation for span lengths was 0.08 ft. There was a range of 0.22-0.26 ft for the footing dimensions. The highest variation for deck width was 0.18 ft. The half-section width had a range of 0.01-0.03 ft.

Table 8. Daylight Photogrammetric Model Measurements

Structural Details/Software	Building Plan	DJI Terra	DroneDeploy
Span A (ft)	103.92	103.90	103.89
Span B (ft)	102.75	102.77	102.75
Span C (ft)	102.75	102.70	102.67
Footing Length (ft)	44.25	44.03	44.01
Footing Width (ft)	25.00	24.74	24.73
Deck (ft)	33.25	33.07	33.18
Half Section (ft)	15.00	14.97	14.99

As shown in. Figure 42, the photogrammetric model allowed a visual inspection of the conditions of the Rip Rap system located at the beginning of the bridge at bent 1.

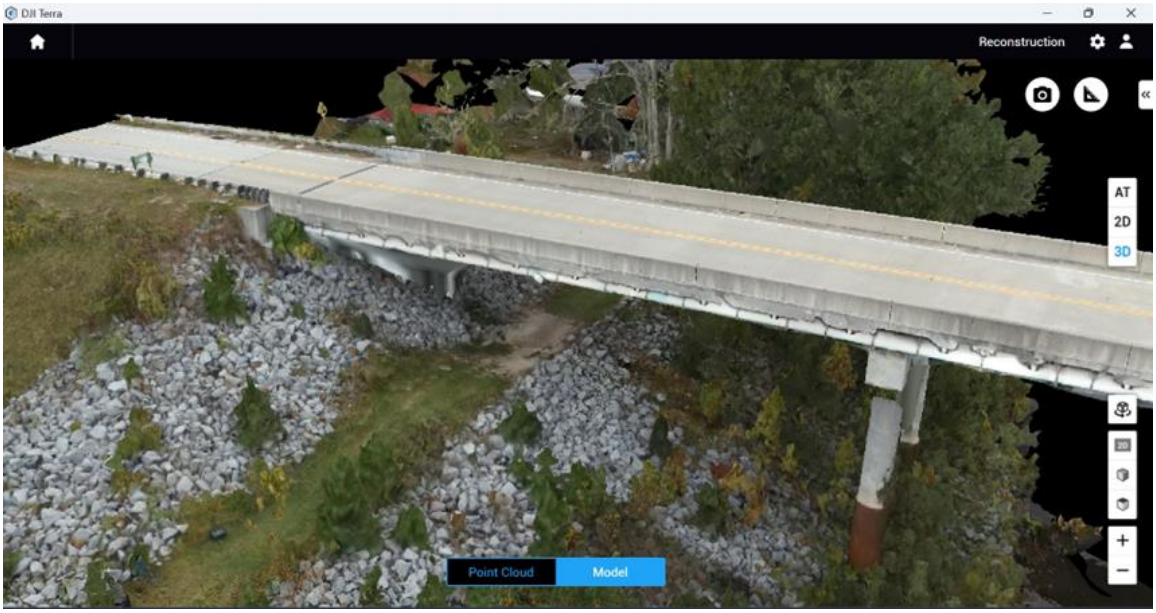

Figure 42. Rip Rap at the Beginning of the Bridge in DJI Terra

6.2.2 Photogrammetric Model in Poor Light Conditions

As well as measurements for daylight conditions, a flight was performed in twilight conditions using the same procedures. Figure 43 demonstrates a twilight view of the 3D photogrammetric model in DJI Terra for the Grimesland Bridge.

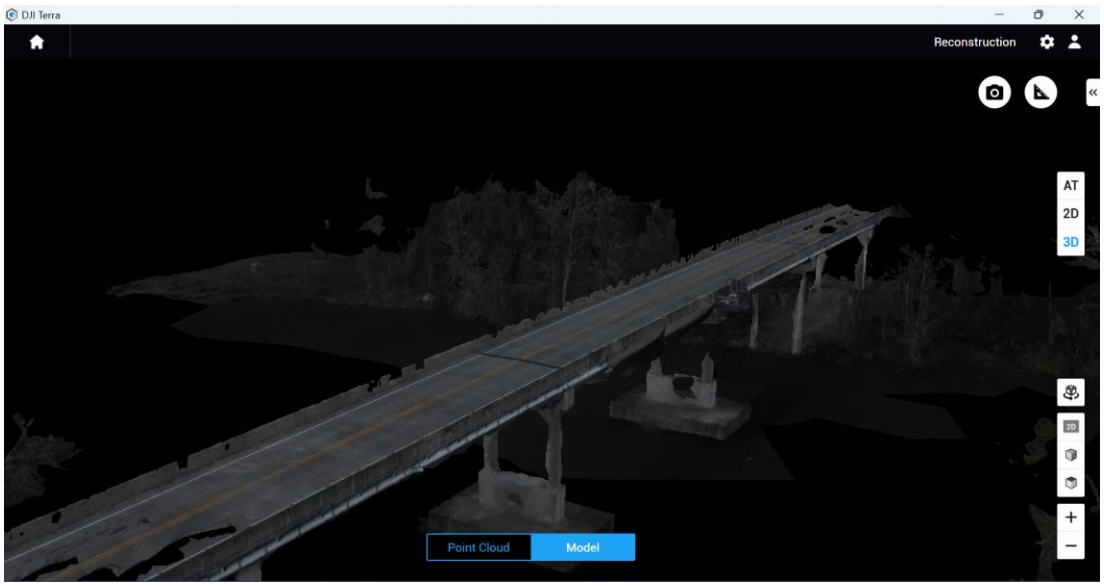

Figure 43. Twilight Photogrammetric Model of the Grimesland Bridge in DJI Terra

For the twilight assessment, Table 9 presents the comparison of linear measurements for three spans, a footing, and a deck section from DJI Terra and DroneDeploy, respectively, with the design values from the structural plans. As for the daylight measurements, the photogrammetric models were compared with the data from the design plans. The greatest twilight variation for span lengths was 0.12 ft, and a range of 0.22-0.31 ft was obtained for the footing dimensions. The highest variation for deck width was 0.34 ft. The observed range for the half-section width was a range of 0.10-0.12 ft.

Table 9. Twilight Photogrammetric Model Measurements

Structural Details/Software	Building Plan	DJI Terra	DroneDeploy
Span A (ft)	103.92	103.89	103.88
Span B (ft)	102.75	102.75	102.75
Span C (ft)	102.75	102.77	102.63
Footing Length (ft)	44.25	44.03	44.02
Footing Width (ft)	25.00	24.69	24.74
Deck (ft)	33.25	33.56	33.59
Half Section (ft)	15.00	14.9	14.88

6.2.3 LIDAR Point Cloud Model

The LIDAR point cloud was processed with the developed error prediction model, which was then imported into Autodesk ReCap Pro, as demonstrated in Figure 44. A Digital Elevation Model was presented with an elevation spectrum range of 55 feet, due to the point cloud model lacking any RGB colors.

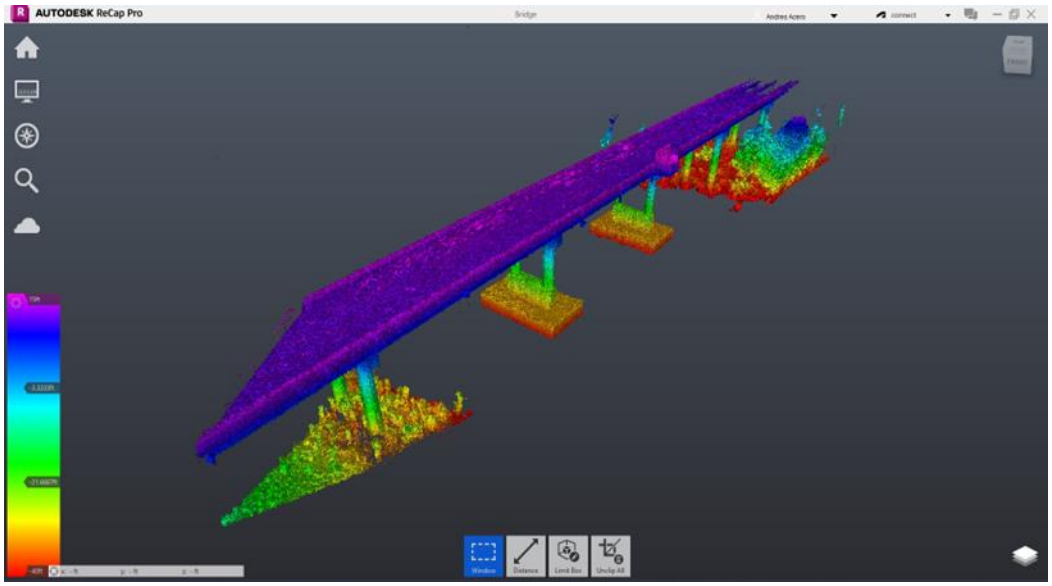

Figure 44. LIDAR Point Cloud Model of the Grimesland Bridge in ReCap Pro

The comparison of the linear dimensions of the structural elements, described in the previous section, with the design values from the structural plans, is presented in Table 10. This

table illustrates that all dimensions are within the 0.1 ft range, while the deck width variation has a range of 0.2-0.3 ft.

Table 10. LIDAR Point Cloud Model Measurements in Autodesk ReCap Pro

Structural Details/Software	Building Plan	ReCap Pro
Span A (ft)	103.92	103.90
Span B (ft)	102.75	102.80
Span C (ft)	102.75	102.80
Footing Length (ft)	44.25	44.20
Footing Width (ft)	25.00	25.00
Deck (ft)	33.25	33.51
Half Section (ft)	15.00	-

6.3 Summary

Three UAS flights were performed at the Grimesland Bridge to verify the measurements from the structural plans for this bridge. Both the DJI Matrice 300 RTK commercial and the customized DJI Matrice 600 Pro UAS systems were utilized to obtain photogrammetric and point cloud models, respectively. Two flights were scheduled using the UAS commercial system: one daylight condition and one twilight condition. The two photogrammetric models showed the greatest differences in comparison with the design plans, for the deck and footing width measurements. In addition, the deck measurement presented a significant variation for both the photogrammetric model, under the twilight condition, and the LIDAR point cloud model.

CHAPTER 7 DISCUSSIONS

7.1 Comparison of UAS Devices

Two UAS systems demonstrating different features were used for this research project, in order to analyze the advantages and qualities of each system. A customized DJI Matrice 600 Pro with a professional LIDAR sensor was used to capture the surface of a construction material pile at low altitudes. In addition, this UAS system was used to collect data from the Grimesland Bridge to compare design information with data obtained from this UAS system. The use of Autodesk Civil 3D allowed volume values to be calculated for the aggregate pile, using the point clouds obtained from the customized UAS LIDAR system. Furthermore, this UAS system was useful for the verification of the design values for the Grimesland Bridge.

The DJI Matrice 300 RTK system collected photogrammetric information for the West Academic Building, the Shipping Containers, the West Water Treatment Building, and the Grimesland Bridge. In addition, the use of the data obtained from this UAS system allowed for the extraction of a point cloud file to be analyzed using both Autodesk ReCap Pro and Autodesk Civil 3D software.

A comparison of the UAS systems is illustrated in Table 11, which shows the contrasts for the two systems' advantages, disadvantages, and characteristics.

Table 11. Comparison of the UAS Systems' Features

UAS System	DJI Matrice 300 RTK	DJI Matrice 600 Pro
Flight Control Method	Automatic	Manual
Data Type	Photogrammetry	Point Cloud
Data Collection	Image camera	LIDAR sensor
Measuring Time	Low	Low
Measuring Effort	Low	Low
Processing Time	High	High
Processing Effort	High	Low
Visual Inspections	Possible	Not possible

7.2 Comparison of UAS Linear Measurements

Linear measurements were performed and compared with the existing known design data to verify the DJI Matrice 300 RTK commercial UAS system's features, prior to performing the primary measurements involving the field inspection of the Grimesland Bridge. The West Academic Building and the shipping containers were measured and compared, with the first site using the design plans and the second site using the factory data sheet. After determining the specified linear measurements using different photogrammetric and point cloud software, the error percentages were obtained. The UAS system measurements in comparison with the design data are shown in Table 12 as a percentage of error.

Table 12. Percentage of Error for the West Academic Building

	% Error						
Location / Method	N(1-4)	N(4-8)	N(8-11)	E(A-E)	E(E-H)	S	W
DJI Terra 2D	-0.74%	-0.09%	-0.10%	0.11%	0.01%	-0.01%	-0.05%
DJI Terra 3D	-0.15%	-0.09%	-0.05%	0.11%	-0.04%	0.10%	0.02%
Drone Deploy	-0.06%	-0.05%	-0.06%	-0.05%	-0.07%	-0.02%	-0.03%
Autodesk Civil 3D	-0.20%	-0.13%	-0.10%	0.07%	-0.09%	0.08%	-0.00%

In the West Academic Building comparison, the highest percentage of error was -0.74% using DJI Terra in 2D view, for side N (1-4). This value shows a high degree of accuracy for certain construction tasks, for example, verification or inspection of structures. Although this value is still unacceptable due to the high degree of accuracy necessary for design and construction, it generates significant possibilities for future research.

For side N (1-4) of the building, the wall's shadow caused a high contrast that did not allow the photogrammetric model to yield a uniform surface in comparison with the other sides of this building. In addition, due to the altitude of the UAS flight performed above ground level (250 ft), the model presents irregularities in the mosaic processing for this side of the building. The highest zoom level was employed for the DJI Terra 2D view, as shown in Figure 45.

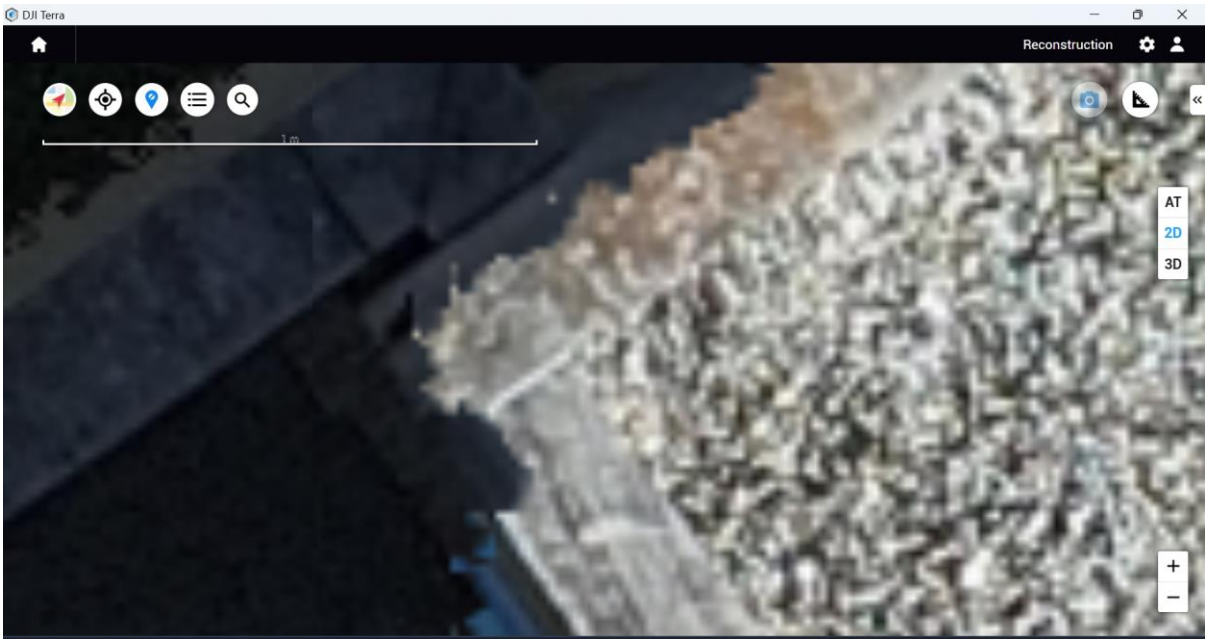

Figure 45. Close-up View of the Corner of Side N(1-4) Using DJI Terra 2D View

The range of percentage of error obtained for shipping containers was higher in the height measurements for all software utilized (-0.94% to -4.21%), as demonstrated in Table 13 and

Table 14. This finding was believed to be due to surface irregularities that did not allow for more accurate results. In addition, objects surrounding the containers interfered with the UAS flight area that was being assessed.

Table 13. Percentages of Error for Shipping Containers Type 40'Dry

Method \ Dimension		% Error Length	% Error Width	% Error Height
Factory Data		-	-	-
DJI Terra	2D	-0.25%	-0.75%	-3.16%
	3D	-0.25%	-0.75%	-4.21%
Drone Deploy		-0.25%	-0.75%	-2.63%
Autodesk Civil 3D		-0.75%	-0.62%	-2.74%

Table 14. Percentages of Error for Shipping Container Type 45'Dry

Method \ Dimension		% Error Length	% Error Width	% Error Height
Factory Data		-	-	-
DJI Terra	2D	-0.27%	-1.13%	-1.41%
	3D	-0.27%	-1.13%	-1.18%
Drone Deploy		-0.27%	-1.13%	-0.94%
Autodesk Civil 3D		0.00%	-0.62%	-1.88%

7.3 Comparison of UAS Volume Measurements

For the three volume measurement methods developed, the comparison between the results and procedures to obtain surveying data for the bulk pile, is presented in Table 15. The surface generated using the full point cloud data, obtained from the customized UAS system, presented closer similarity to the real physical surface in comparison with the surfaces created using the GPS points and the extracted point cloud data. However, since the true base surface is unmeasurable and can even change under the weight of the pile, the true volume and accuracy cannot be determined and only the volume differences between the three measurement methods

can be observed (Guan et al., 2022b). While the UAS methods can effectively reduce the labor required for measurements, the full point cloud method does require a longer time and more effort for data processing.

Table 15. Comparison of Volume Measurement Methods of Bulk Pile

Measurement Method	Surveying GPS	Extracted Point Cloud	Full Point Cloud
Volume (Cubic Yard)	351.53	354.84	292.39
Volume Difference	-	+1%	-17%
% Difference	-	Low	High

For the West Water Treatment Building, the resulting values shown in Chapter 5, Table 7 presented significant differences due to the limitation when determining a point of reference to create an area to be analyzed by the photogrammetric models. Additionally, it was also challenging to determine a surface in the point cloud model because a standard elevation was not established for this structure to use as a reference to create a uniform ground surface. However, it should be noted that the specific purpose for measuring the volume of this building, and other sites located on the ECU West Academic Campus, was to evaluate the commercial UAS system's features and performance. In the photogrammetric models obtained for the WWTB, it was not necessary to generate a surface because the area covered to calculate the volume included a tridimensional axis (X, Y, Z).

7.4 Comparison of UAS Bridge Inspection

Table 16 presents the percentage of errors obtained using the photogrammetric model (daylight and twilight conditions) and the LIDAR point cloud model. The results demonstrate that most UAS measurements are within 1% of the design values as compared to the structural plans of the bridge. The majority of the variations are marginally smaller than the design values. The highest errors in the photogrammetric models involved the footing width at -1.08% (daylight

using DroneDeploy) and 1.24% (twilight using DJI Terra). In the point cloud model, the greatest error is associated with the deck result of 0.78%.

Table 16. Error Percentages of the Measurements Using Different Software

Structural Details/Software	DJI Terra Daylight	Drone Deploy Daylight	DJI Terra Twilight	Drone Deploy Twilight	Autodesk ReCap Pro
Span A (ft)	-0.02%	-0.03%	-0.03%	-0.04%	-0.02%
Span B (ft)	-0.02%	0.00%	0.00%	0.00%	0.05%
Span C (ft)	-0.05%	-0.08%	0.02%	-0.12%	0.05%
Footing Length (ft)	-0.50%	-0.54%	-0.50%	-0.52%	-0.11%
Footing Width (ft)	-1.04%	-1.08%	-1.24%	-1.04%	0.00%
Deck (ft)	-0.54%	-0.21%	0.93%	1.02%	0.78%
Half Section (ft)	-0.20%	-0.07%	-0.67%	-0.80%	-

The measurement error for footing width is -1.08% in the daylight condition using DroneDeploy. It represents a decrease of approximately one-quarter foot, compared with the design value, which is much higher than the errors of other measurements for daylight conditions for photogrammetric models. Because of the possible effects of wave action, buoyancy, debris striking, or abrasion around the foundations, the images obtained using the commercial UAS system possess significant alterations. Thus, it will be necessary to perform additional verifications and inspections as a means to assure the structural integrity of the bridge's structures. With the use of the UAS photogrammetric model in the daylight condition, it was possible to visually verify other systems and elements surrounding the bridge, such as drainage or erosion control systems like the Rip Rap system, located at the beginning of the bridge, as shown in Chapter 6, Figure 42.

The footing width error of -1.24% obtained in the twilight condition using DJI Terra, compared with the design value, is the greatest error in this research to perform a field inspection. Irregularities in the edges of the concrete on one or both sides of the bridge, in

twilight conditions, resulted in measurement variations in comparison to the design plan values. In this model, the borders of this bridge were difficult to determine due to the lack of natural light. Figure 46 shows the contrast between the daylight and twilight models, which demonstrates irregularities on both edges of the bridge. In addition, the performance of visual inspections using the model under twilight conditions is more complicated due to the quality of the imagery generated in this condition. For example, for verification of the actual status of the structures, the unfilled regions at multiple locations in the deck might omit important details, such as fatigue and pavement cracks.

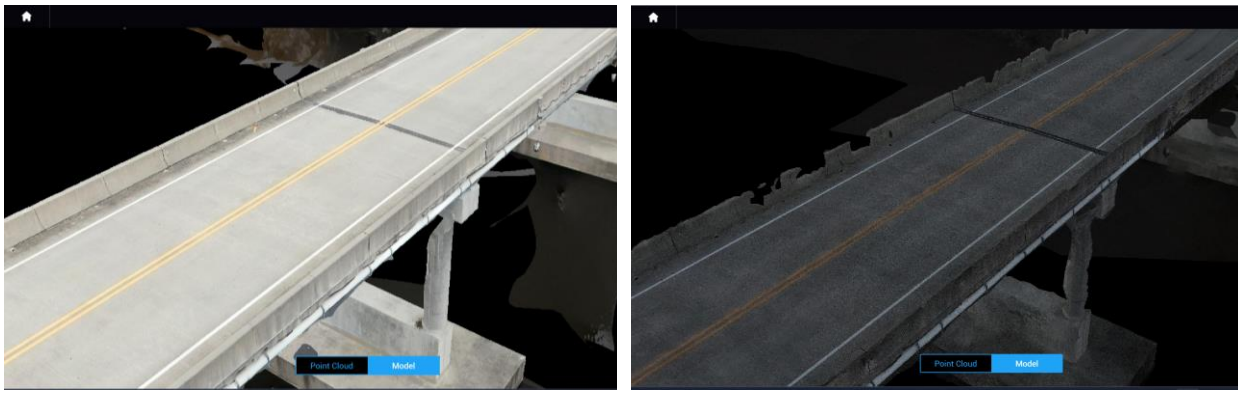

(a) Model in Daylight Conditions (b) Model in Twilight Conditions

Figure 46. Expanded View of the Deck in Photogrammetric Models

Figure 47 and Figure 48 represent the percentages of error obtained using daylight and twilight conditions for each element measured as compared with the design data. The figures show that in both conditions, the footing width denotes the greatest variation.

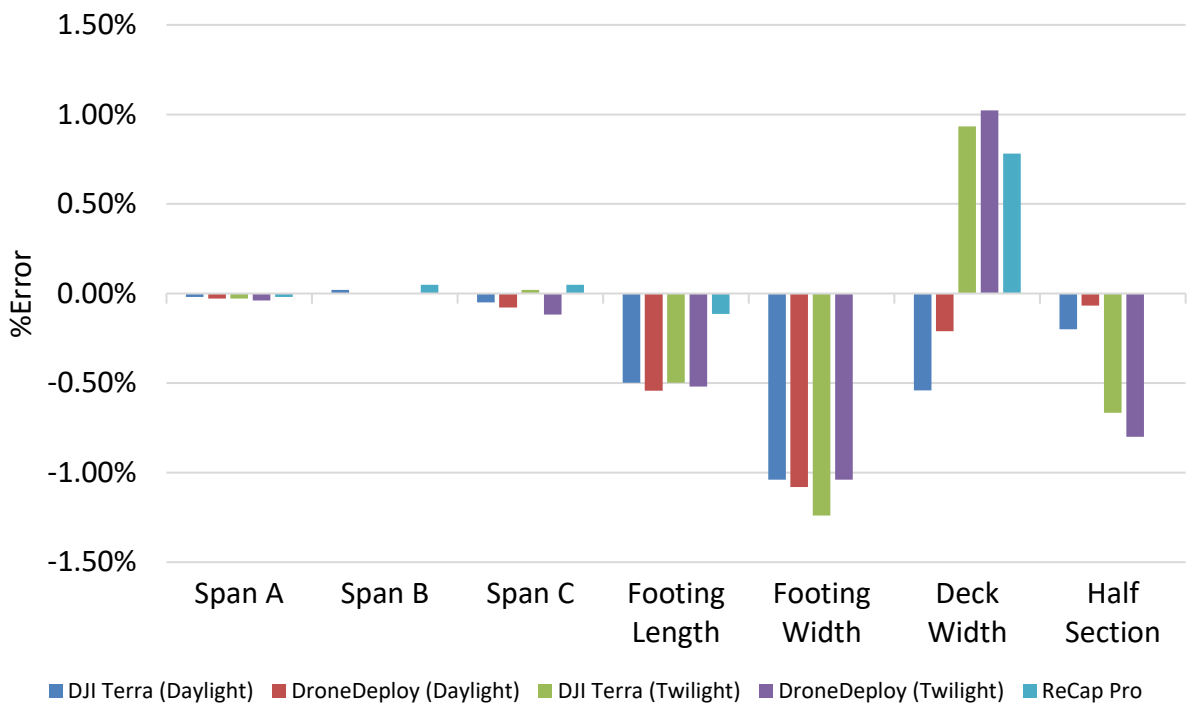

Figure 47. Illustration of Percentage of Error in UAS Measurements by Bridge Structure

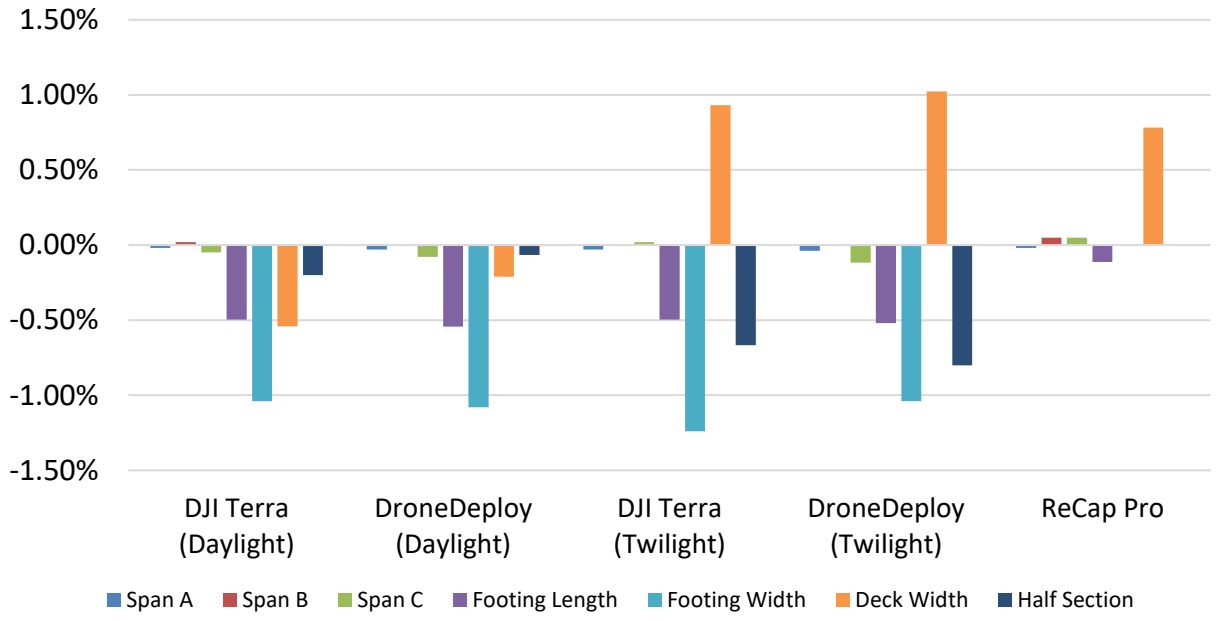

Figure 48. Illustration of Percentage of Error in UAS Measurements by Lighting Condition

CHAPTER 8 CONCLUSIONS AND RECOMMENDATIONS

The construction industry worldwide is experiencing new challenges due to the technological advancement and optimization of previously unavailable techniques that enhance the development of construction projects. One of the fields facing important changes is surveying because the traditional methods to obtain onsite information have exhibited limitations regarding the quality of the data. These limitations involved human errors, exposure to inclement conditions related to climate variations, and accessibility issues for some construction sites. Unmanned Aircraft Systems (UAS) have been implemented for surveying and onsite inspection tasks for the purpose of optimizing costs, labor, and time.

For this project, the findings of current UAS uses in construction spanning the years 2016-2021 were analyzed for a total of 95 papers, from a list of 21 journals and conference proceedings. This literature review revealed that the number of studies using UAS for construction is significantly increasing; and the United States leads in this research focusing on inspection, surveying, algorithms, and operations involving buildings, bridges, and roads.

This study developed different onsite experiments using UAS for the purpose of verifying the linear dimensions at two different sites; comparing the data obtained using traditional surveying with the data obtained using UAS; the creation of volume models from a bulk pile; and investigating UAS performance for field inspections. Two UAS were utilized: one is a customized LIDAR UAS with a LIDAR sensor which was used to create point cloud models, and the other is a commercial UAS employed for the creation of photogrammetric models.

8.1 Benefits Concerning UAS Uses in Construction

As demonstrated in this research study, the use of UAS devices was easier and did not require as much time as traditional methods of surveying, such as the GPS used to obtain volume calculations for the aggregate pile at the NCDOT. UAS offers safety for pilots when attempting to access hazardous construction sites. Since the commercial UAS was programmed automatically, the pilot only needs to define flight standards in order to perform the flight.

Using point cloud data obtained from UAS allowed this study to create more accurate models due to the quantity of points generated, in comparison with GPS. As shown in Chapter 5, the surface generated using full point cloud data was more irregular than the surfaces generated using GPS and extracted point cloud data. Thus, the full point cloud results were more similar to the real surface.

For construction field inspection, although the maximum percentage of error in the model generated under daylight conditions was -1.08%, a generally acceptable degree of accuracy was exhibited. In addition, photogrammetric models can provide high-quality pictures for visual inspection of other bridge components, such as the assessment of the Rip Rap at the beginning of the Grimesland Bridge.

8.2 Limitations Concerning UAS Uses in Construction

The data obtained using both UAS required significant processing effort and time. The performance of the UAS flight, when using the customized UAS having manual controls, depends on the skills of the pilot.

For some photogrammetric models, shadow effects caused a high contrast that did not allow the photogrammetric model to yield a uniform surface. Due to the varied altitudes of the

UAS flights performed above ground level, the model presents irregularities in the mosaic processing. Occasionally, surface irregularities did not allow for more accurate measurement results.

Because of the possible effects of wave action, buoyancy, debris striking, or abrasion around the foundations, the images obtained using the commercial UAS possess significant alterations. The performance of visual inspections using the model under twilight conditions is more complicated due to the quality of the imagery generated in this condition.

8.3 Recommendations for Future Research Involving UAS Uses in Construction

This research only employed two types of UAS: photogrammetric and LIDAR point cloud technologies. However, other UAS involving different sensing technologies might provide more data in order to analyze UAS efficiency for specific construction purposes such as verification, calculation, and inspection. Other types of sensing technologies for future research could include thermal imaging, video footage, and multispectral images.

UAS data was compared with GPS data in this study. It is recommended that other traditional surveying instruments be utilized for comparison purposes. For example, future research could involve total station, theodolite, and/or levels.

The accuracy of elevations was not assessed in this study. This information is significant in order to improve the effectiveness of UAS onsite inspections. Therefore, it is recommended that elevations should be analyzed in future research using UAS.

REFERENCES

Adjidjonu, D. and J. Burgett (2019). Optimal UAS Parameters for Aerial Mapping and Modeling. *Proceedings of the 55th ASC Annual International Conference Proceedings, Denver, CO, USA*.

Albeaino, G. and M. Gheisari (2020). "Trends, benefits, and barriers of unmanned aerial systems in the construction industry: a survey study in the United States." *Journal of Information Technology in Construction* 26: 84-111.

Albeaino, G., M. Gheisari and B. Franz (2019). "A systematic review of unmanned aerial vehicle application areas and technologies in the AEC domain." *Journal of Information Technology in Construction* 24: 381-405.

Asadi, K. and K. Han (2020). An integrated aerial and ground vehicle (UAV-UGV) system for automated data collection for indoor construction sites. *Construction Research Congress 2020: Computer Applications*, American Society of Civil Engineers Reston, VA.

Asadi, K., A. K. Suresh, A. Ender, S. Gotad, S. Maniyar, S. Anand, M. Noghabaei, K. Han, E. Lobaton and T. Wu (2020). "An integrated UGV-UAV system for construction site data collection." *Automation in Construction* 112: 103068.

Bang, S. and H. Kim (2020). "Context-based information generation for managing UAV-acquired data using image captioning." *Automation in Construction* 112(103116): 1-10.

Bang, S., H. Kim and H. Kim (2017). "UAV-based automatic generation of high-resolution panorama at a construction site with a focus on preprocessing for image stitching." *Automation in Construction* 84: 70-80.

Bashmal, L., Y. Bazi, H. AlHichri, M. M. AlRahhal, N. Ammour and N. Alajlan (2018). "Siamese-GAN: Learning Invariant Representations for Aerial Vehicle Image Categorization." *Remote Sensing* 10(2): 351.

Bianchi, E., A. L. Abbott, P. Tokekar and M. Hebdon (2021). "COCO-bridge: structural detail data set for bridge inspections." *Journal of Computing in Civil Engineering* 35(3): 04021003.

Chen, K., G. Reichard and X. Xu (2019). Opportunities for Applying Camera-Equipped Drones towards Performance Inspections of Building Facades. Computing in Civil Engineering 2019: 113-120.

Chen, M., A. Feng, K. McCullough, P. B. Prasad, R. McAlinden and L. Soibelman (2020). "3D Photogrammetry Point Cloud Segmentation Using a Model Ensembling Framework." *Journal of Computing in Civil Engineering* 34(6): 04020048.

Chen, S., D. F. Laefer, E. Mangina, S. I. Zolanvari and J. Byrne (2019). "UAV bridge inspection through evaluated 3D reconstructions." *Journal of Bridge Engineering* 24(4): 05019001.

Dorafshan, S., R. J. Thomas and M. Maguire (2018). "Fatigue crack detection using unmanned aerial systems in fracture critical inspection of steel bridges." *Journal of bridge engineering* 23(10): 04018078.

Dupont, Q. F. M., D. K. H. Chua, A. Tashrif and E. L. S. Abbott (2017). "Potential Applications of UAV along the Construction's Value Chain." *Procedia Engineering* 182: 165-173.

Duque, L., J. Seo and J. Wacker (2018). "Bridge deterioration quantification protocol using UAV." *Journal of Bridge Engineering* 23(10): 04018080.

Elmekati, A. H., R. Dannenberg and N. M. Ghanem (2019). Geotechnical Health Assessment of Roadway Embankment Using Airborne LiDAR. *Geo-Congress 2019: Embankments, Dams, and Slopes*, American Society of Civil Engineers Reston, VA.

Eschmann, C. and T. Wundsam (2017). "Web-Based Georeferenced 3D Inspection and Monitoring of Bridges with Unmanned Aircraft Systems." *Journal of Surveying Engineering* 143(3): 04017003.

Franke, K. W., K. M. Rollins, C. Ledezma, J. D. Hedengren, D. Wolfe, S. Ruggles, C. Bender and B. Reimschiissel (2017). "Reconnaissance of Two Liquefaction Sites Using Small Unmanned Aerial Vehicles and Structure from Motion Computer Vision Following the April 1, 2014 Chile Earthquake." *Journal of Geotechnical and Geoenvironmental Engineering* 143(5): 04016125.

Fu, B., M. Liu, H. He, F. Lan, X. He, L. Liu, L. Huang, D. Fan, M. Zhao and Z. Jia (2021). "Comparison of optimized object-based RF-DT algorithm and SegNet algorithm for classifying Karst wetland vegetation communities using ultra-high spatial resolution UAV data." *International Journal of Applied Earth Observation and Geoinformation* 104: 102553.

Google (2022). East Carolina University West Research Campus View in 2D.

Guan, S., Y. Huang, G. Wang, H. Sirianni and Z. Zhu (2022). "An Error Prediction Model for Construction Bulk Measurements Using a Customized Low-Cost UAS-LIDAR System." *Drones* 6(7): 178.

Ham, S. W., H.-C. Park, E.-J. Kim, S.-Y. Kho and D.-K. Kim (2020). "Investigating the influential factors for practical application of multi-class vehicle detection for images

from unmanned aerial vehicle using deep learning models." *Transportation Research Record* 2674(12): 553-567.

Ham, Y. and M. Kamari (2019). "Automated content-based filtering for enhanced vision-based documentation in construction toward exploiting big visual data from drones." *Automation in Construction* 105: 102831.

Hou, Y., R. Volk, M. Chen and L. Soibelman (2021). "Fusing tie points' RGB and thermal information for mapping large areas based on aerial images: A study of fusion performance under different flight configurations and experimental conditions." *Automation in Construction* 124: 103554.

Inzerillo, L., G. Di Mino and R. Roberts (2018). "Image-based 3D reconstruction using traditional and UAV datasets for analysis of road pavement distress." *Automation in Construction* 96: 457-469.

Irizarry, J. and D. B. Costa (2016). "Exploratory Study of Potential Applications of Unmanned Aerial Systems for Construction Management Tasks." *Journal of Management in Engineering* 32(3): 05016001.

Jiang, Y. and Y. Bai (2020). Determination of Construction Site Elevations Using Drone Technology. Construction Research Congress 2020: 296-305.

Jiang, Y. and Y. Bai (2020). "Estimation of Construction Site Elevations Using Drone-Based Orthoimagery and Deep Learning." *Journal of Construction Engineering and Management* 146(8): 04020086.

Jiang, Y. and Y. Bai (2021). "Low-High Orthoimage Pairs-Based 3D Reconstruction for Elevation Determination Using Drone." *Journal of Construction Engineering and Management* 147(9): 04021097.

Jiang, Y., Y. Bai and S. Han (2020). "Determining Ground Elevations Covered by Vegetation on Construction Sites Using Drone-Based Orthoimage and Convolutional Neural Network." *Journal of Computing in Civil Engineering* 34(6): 04020049.

Kamari, M. and Y. Ham (2018). Automated Filtering Big Visual Data from Drones for Enhanced Visual Analytics in Construction. Construction Research Congress 2018: 398-409.

Kim, P., J. Park, Y. K. Cho and J. Kang (2019). "UAV-assisted autonomous mobile robot navigation for as-is 3D data collection and registration in cluttered environments." *Automation in Construction* 106: 102918.

Kim, S., Y. Gan and J. Irizarry (2021). "Framework for UAS-Integrated Airport Runway Design Code Compliance Using Incremental Mosaic Imagery." *Journal of Computing in Civil Engineering* 35(2): 04020070.

Kim, S. and K. Kim (2021). "Systematic Tertiary Study for Consolidating further Implications of Unmanned Aircraft System Applications." *Journal of Management in Engineering* 37(2): 03120001.

Li, Y. and C. Liu (2019). "Applications of multirotor drone technologies in construction management." *International Journal of Construction Management* 19(5): 401-412.

Liu, D., X. Xia, J. Chen and S. Li (2021). "Integrating Building Information Model and Augmented Reality for Drone-Based Building Inspection." *Journal of Computing in Civil Engineering* 35(2): 04020073.

Liu, Y., J. K. W. Yeoh and D. K. H. Chua (2020). "Deep Learning - Based Enhancement of Motion Blurred UAV Concrete Crack Images." *Journal of Computing in Civil Engineering* 34(5): 04020028.

Martinez, J. G., G. Albeaino, M. Gheisari, W. Volkmann and L. F. Alarcón (2021). "UAS Point Cloud Accuracy Assessment Using Structure from Motion Based Photogrammetry and PPK Georeferencing Technique for Building Surveying Applications." *Journal of Computing in Civil Engineering* 35(1): 05020004.

Martinez, J. G., M. Gheisari and L. F. Alarcón (2020). "UAV Integration in Current Construction Safety Planning and Monitoring Processes: Case Study of a High-Rise Building Construction Project in Chile." *Journal of Management in Engineering* 36(3): 05020005.

Omar, T. and M. L. Nehdi (2017). "Remote sensing of concrete bridge decks using unmanned aerial vehicle infrared thermography." *Automation in Construction* 83: 360-371.

Park, J., P. Kim, Y. K. Cho and J. Kang (2019). "Framework for automated registration of UAV and UGV point clouds using local features in images." *Automation in Construction* 98: 175-182.

Phillips, S. and S. Narasimhan (2019). "Automating data collection for robotic bridge inspections." *Journal of Bridge Engineering* 24(8): 04019075.

Pi, Y., N. D. Nath and A. H. Behzadan (2021). "Detection and Semantic Segmentation of Disaster Damage in UAV Footage." *Journal of Computing in Civil Engineering* 35(2): 04020063.

Seo, J., L. Duque and J. Wacker (2018). "Drone-enabled bridge inspection methodology and application." *Automation in construction* 94: 112-126.

Shang, Z. and Z. Shen (2018). Real-time 3D reconstruction on construction site using visual SLAM and UAV. *Construction Research Congress 2018*.

Shojaei, A., H. I. Moud and I. Flood (2018). "Proof of Concept for the Use of Small Unmanned Surface Vehicle in Built Environment Management." *Construction Research Congress 2018*: 116-126.

Siebert, S. and J. Teizer (2014). "Mobile 3D mapping for surveying earthwork projects using an Unmanned Aerial Vehicle (UAV) system." *Automation in Construction* 41: 1-14.

Solutions, A. B. G. F. F. (2016). Airfreight Container Specifications. Australia.

Wang, L. and J. Li (2021). "Fast Blur Detection Algorithm for UAV Crack Image Sets." *Journal of Computing in Civil Engineering* 35(6): 04021029.

Xiao, Y., V. R. Kamat and S. Lee (2018). Monitoring Excavation Slope Stability Using Drones. Construction Research Congress 2018: 169-179.

Zhou, Z., J. Gong and M. Guo (2016). "Image-Based 3D Reconstruction for Posthurricane Residential Building Damage Assessment." *Journal of Computing in Civil Engineering* 30(2): 04015015.

Zhou, Z., J. Irizarry and Y. Lu (2018). "A Multidimensional Framework for Unmanned Aerial System Applications in Construction Project Management." *Journal of Management in Engineering* 34(3): 04018004.